Radiocommunications Agency
Ministry of Economic Affairs

Method for measuring the EMI radiation of wind turbines in relation to the LOFAR radio telescope

Colophon

To	Coordination Committee Covenant
From	Radiocommunications Agency
Number	V1.0
Date	08 September 2017
Contributors	ASTRON INAF Movares Radiocommunications Agency Netherlands
Editor in chief	Radiocommunications Agency

Contents

Management summary

The Radiocommunications Agency has been tasked to develop the method to measure low EMI radiation from wind turbines in relation to the LOFAR radio telescope as, described in the covenant between ASTRON and the initiators of the windfarm "Drentse Monden and Oostermoer". The method was developed in close cooperation with the signatories of the covenant.

After review of several methods, a victim oriented approach has been chosen, leading to a measurement method consisting of an array of multiple receivers and antennas and a software processing solution. The measurement challenges, the different possible methods and the final choice are all discussed.

A design based on this final choice, the measurement criteria and the required sensitivity are described. The theoretical minimum configuration was verified with a representative test signal using part of the LOFAR radio telescope and processing software specifically developed for this task.

For measuring the -35 dB level for the whole practical frequency band of LOFAR (30-240 MHz), a minimum number of 18 antenna elements with an array size of 100 m is required to obtain sufficient receiving sensitivity and the ability to filter out unwanted signals, mainly the normal astronomical objects. The distance of the array from the wind turbine under test needs to be roughly 1000 m. The minimum observation time is 1000 seconds, provided appropriate antennas are used. Measuring the -50 dB level down to 30 MHz involves about 96 antennas and 7200 s integration time with an array diameter of 150 m at 1 km distance, when we assume a directionality better than 0 dB and a gain towards the turbine better than -8 dBi for the antenna elements.
A vertically polarised log-periodic antenna or other antenna with suppression in the direction of the zenith and high elevation angles, such as a (combination of) vertical monopole(s), is a suitable antenna element for a practical implementation. Using such an antenna element will aid in decreasing the number of antenna elements. It is up to a system designer to make a final choice when implementing the method, because bandwidth and observation time depends on the choice.

The method requires a calibrated radio beacon to ensure that any scalings of the absolute results due to local radio propagation peculiarities, antenna/receiver properties, and the data reduction method are measured and compensated for.

Being an imaging radio array itself, one could in principle use (components of) LOFAR to perform the measurements. This would imply building a wind turbine about 1 km from a remote LOFAR station, or at one of the designated wind turbine sites closest to the LOFAR core, at a distance of approximately 5 km. It turns out that a LOFAR station by itself is not able to do certification observations all the way down to 30 MHz. The full LOFAR core may be able to do this, but to establish definitively whether this is possible requires more detailed simulation work, which we have not yet been able to conduct.

This report describes the background, principles and validation of the recommended measurement method as required by the covenant. The implementation will require a separate engineering project with challenging choices, especially for the low frequencies.

The report has been reviewed and commented on our request by Dr. Hawlitschka from the Fraunhofer Institute and P.C. Hoefsloot from TNO, and their valuable suggestions have led to an improved final text.

Introduction

In 2016 the Radiocommunications Agency / Agentschap Telecom performed research into the possible disturbance of the LOFAR radio telescope by a planned windfarm in Drentse Monden. The results of this research can be found in the report "Verstoring van het elektromagnetische milieu ter plaatse van de LOFAR kern door het wind turbinepark Drentse Monden en Oostermoer", also called the Interference Report[10].
The self-radiated EMC energy, apart from the total possible radiated EM energy from a wind turbine (radiation & reflection), showed already to be an operational risk for the extreme sensitive LOFAR radio telescope. The exact value and calculation method can be found in that report.

After discussion between the involved parties it was agreed that the maximum allowed radiated EM energy needs to be at least 35dB below the reference value used in the interference report in order to avoid too much operational interference. This value was set as a condition in a covenant between ASTRON and the initiators of the windfarm for the construction of the windfarm.
If the interference stays 50dB below the reference value there should be no operational limitation for the windfarm.

As part of this agreement the Radiocommunications Agency was tasked, in cooperation with the involved parties to develop a method to measure and possibly safeguard (see article 8 of the covenant) the radiation from the wind turbine in order to validate and enforce the -35dB and reliably measure the -50dB value to establish in which operational category the wind farm belongs.

This report contains an analysis of requirements for such a measurement methods and describes a method to achieve this goal. This method is tested, validated and described in detail, to the extent that an implementation of the measurement setup may be constructed.

Reading guide
Chapter one first explains the challenges of measuring EMI from wind turbines directly followed by the solution we found. The rest of the report from chapter two to seven describes the research process and considered choices we made. The report ends with the main conclusion about the method and the researchers' recommendation for implementation.

1 Problem definition and solution

The measurement problem described in this report involves the measurement of very low level EMI emission from a wind turbine in the presence of interfering sources. For this we need sensitivity but there is also a need to subtract interferers. The main interferers are the normal astronomical sky objects but also "normal" EMI is present in the measurement scenario.
Part of the measurement problem is also that with regular measurement equipment the required sensitivities cannot be achieved.

For solving such a measurement question we need both resolution in the direction of the wind turbine under test and the ability to remove unrelated interferers. After rejecting several methods as described in annex E the solution was found in an array of antennas and multiple receivers. The measurement situation and layout is depicted in figure 1.1

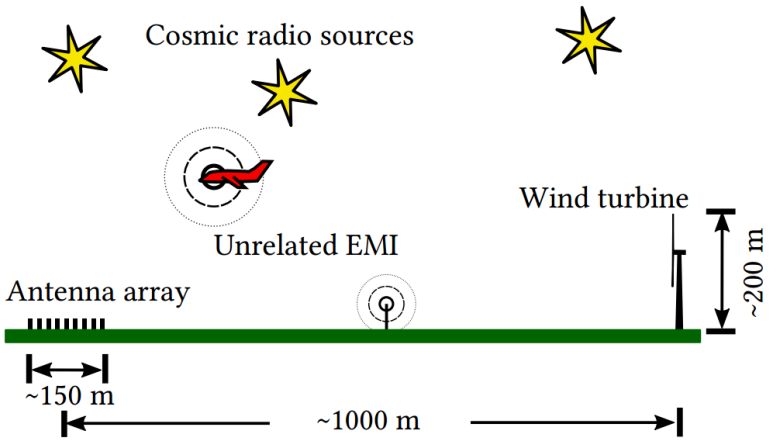

Figure 1.1: Graphical presentation of measurement situation

Because the layout and specific data processing of the victim plays a role in the interference scenario we decided to emulate these typical parts of the victim.

This requires a multichannel receiving system and associated antennas and low Noise Amplifiers (LNA´s).
The design of parts of LOFAR can be used for this. The processing can be done using methods used for the processing of LOFAR data. In order to achieve the required sensitivity and elimination of interferers, processing of data is necessary.

Despite the fact that this solution requires non-standard hardware, it is technically the only possible option to obtain the required sensitivity, to cope with irregularities in the field strength, and to perform a measurement in a realistic EMI scenario as may be encountered near a wind turbine.

The footprint of the antenna array is based on the frequency and measurement distance and has to be designed in such a way that sufficient compensation for the interference pattern as described in section 6.2 takes place.

The proposed solution needs on-site calibration because the antenna system covers a large area and its placement is somewhat different every time it is deployed. Also

environmental conditions vary between deployments and observations. It eliminates also all short term uncertainties in for example the receivers. Calibration is needed before the measurement but is also required during the measurement. A source deployed at 100 m height consisting of a small RF generator and antenna can be placed on for example the wind turbines nacelle. The unit described in annex B can be used as an example.

The calibration source may be placed on the wind turbines nacelle. During the measurement it is necessary to turn the calibration source on and off. For a background noise measurement the wind turbine should be stopped and the medium voltage switched off timely close to the operating measurement.

This method was further developed, and a field test was performed of which is described in Annex E together with the design considerations. Implementation issues are described in annex A.

The minimum number of antennas required to measure wind turbine interference with a signal-to-noise ratio of at least 10 are given in table 1.1. These configurations are derived from simulations using selection criteria described in section 7. Note that the number of antennas that are required depends strongly on the type of antenna used, particularly the antenna's gain towards the wind turbine under test, and the relative directivity (gain towards wind turbine divided by the mean gain elsewhere on the hemisphere). In this table we assumed a directionality better than 0 dB and a gain towards the turbine better than -8 dBi. Because of the enormous relative frequency range, it may be economically attractive to operate more than one array, for example one from 30-80 MHz, and another one from 100-240 MHz.

Array designs aimed to measure -35 and -40 dB levels below the reference level based on CISPR11 are mainly defined by their ability to subtract and reject sources from elsewhere, while the -45 dB and -50 dB capable configurations are defined by the thermal noise.

Required level below norm value	Required # of antennas at 30 MHz with array size D	Required # of antennas at 60 MHz with array size D	Required # of antennas at 120 MHz with array size D	Required observation time (s)
-35	18 (D=100 m)	18 (D=75 m)	18 (D= 75 m)	1000
-40	24 (D=100 m)	24 (D=75 m)	18 (D=100 m)	1000
-45	60 (D=150 m)	36 (D=75 m)	24 (D= 75 m)	1800
-50	96 (D=150 m)	60 (D=75 m)	36 (D= 75 m)	7200

Table 1.1 number of antennas versus measurement level at 30, 60 and 120 MHz

An array in the shape of a Reuleaux triangle, see figure 1.2 has proven to be the most efficient configuration, an explanation can be found in section 6 and 7.

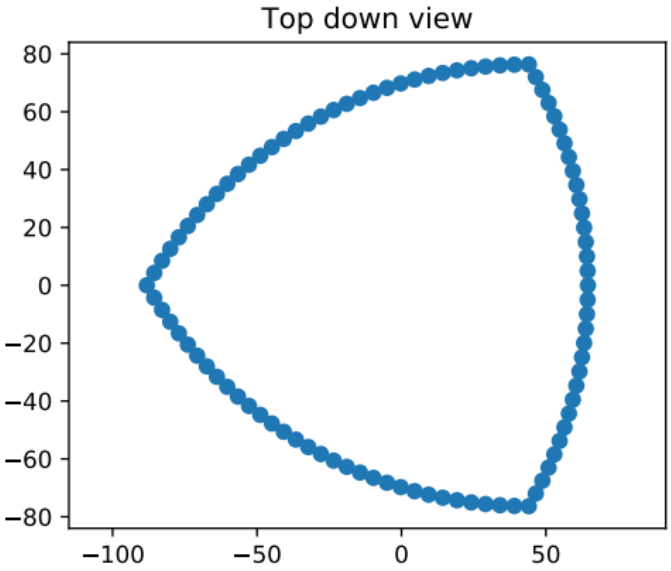

Figure 1.2 Reuleaux triangle configuration for -50dB measurement at 30 MHz

2 Measurement apparatus

The measurement system basically consists of multiple synchronous digital receivers, data storage and processing, this section describes the different parts.

2.1 Data acquisition architecture

The detailed signal path for the data acquisition system is given in figure 2.1

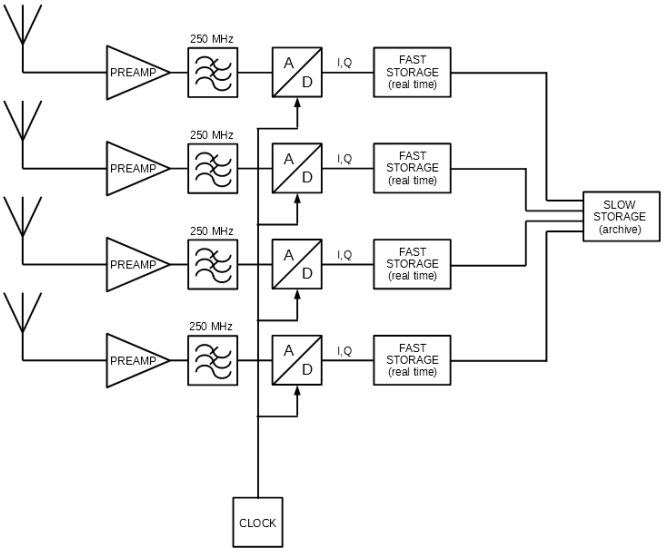

Figure 2.1: Receiver basic architecture

The antennas are connected to preamps to achieve the desired sensitivity in combination with the Analog to Digital Converters (ADC). In front of the ADC an antialiasing filter is placed. The sampling clocks of these AD converters are synchronised through a central clock, this is also called a clock distribution system. The whole spectrum from DC-240 MHz is sampled, each sample could be time tagged but in principle it is sufficient to tag only the start of the registration. The samples are complex IQ (Re/Im).

2.2 18+ element cross-correlating interferometer

An array in the shape of a Reuleaux triangle, see figure 1.2, has proven to be a useful and efficient configuration. An explanation can be found in sections 6 and 7.

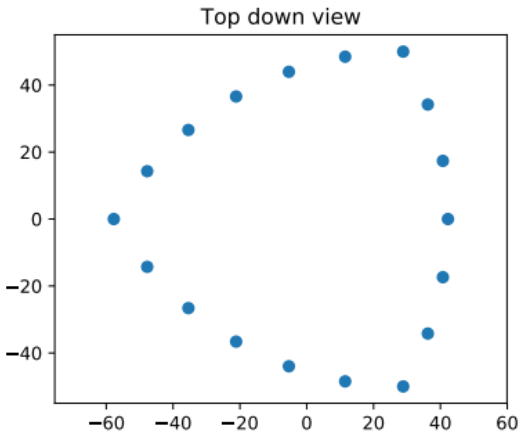

Figure 2.2 Reuleaux triangle

For each antenna the observed band is divided in channels of 1 to 3 kHz wide and the data is averaged to 0.1 to 0.5 seconds time resolution.
This produces the so-called raw visibilities from which the all-sky images can be formed. The raw visibilities need to be processed further in the following way:

- Mark bad data (burst-like interference, narrowband interference, or otherwise unphysical data as such. This stage is called "flagging".
- Average the data in frequency to channels of a few tens to hundreds of kHz to reduce the amount of data, excluding any flagged data from the averaging;
- Calibrate the mean amplitudes and phases of all antennas using the calibration source as well as the brightest sources in the sky.
- Correct the data for these calibration solutions;
- Form and deconvolve an image of the area near the wind turbine, by for example jointly fitting the apparent brightnesses of the wind turbine and the brightest few astrophysical sources, including the Sun.
- Calibrate the absolute brightness scale of the final measurements using the calibration source observations.

The first 3 steps require the most compute power because they operate on un-averaged data.

2.3 Desired antenna properties

The antenna type is not critical for the reliability of the measurement however an antenna with a good relative suppression towards the sky in relation to the lower elevation angles 2,5-5° is preferred because this increases the sensitivity of the whole system and lowers the required number of antennas. An antenna with a good absolute gain towards the wind turbine is required to reduce the total required observation time down to a minimum of 1000 s which is necessary to sufficiently average over short term fluctuations in the wind turbine's interference.
In annex C an example antenna is evaluated, this is an expensive solution and is only included in this report as an example.

2.4 IQ data storage

During measurements a fast storage is needed, SSD's are the obvious choice but these are expensive especially in larger sizes. It is practical to store the content of the SSD to a conventional hard disk (array) after the measurement and free the SSD for the next measurement. This principle is shown in figure 2.1. The data on these disks may be analysed off site.
Here we give an idea of the required disk space at 16bit resolution. When designing a system for 30-240 MHz an IQ sampling rate of 240 MHz is needed (or 500MHz for non IQ). Storage will be done at 16 bit to preserve enough dynamic range between terrestrial transmitters and the thermal noise. This results in 960MB/sec for each receiver or 58GB/minute or 3.5TB/hour. A 96 element array observing for 7200 s total time yields almost 664 TB of raw data.

3 Procedures

The following test procedure should be followed measuring one wind turbine:

Deploy the antenna system in the direction in which the measurement is to be performed, this will be in the direction of the part of the wind turbine facing the victim. The nacelle has the possibility to turn the blades in the direction of the wind so a measurement in more than one direction may be needed. A site survey is needed to indicate which direction is the dominant direction of radiation with the nacelle in different positions. This may be done at a short distance for example at 100 m since it is no absolute field strength measurement. This dominant direction needs to face the direction of the victim so a worst case measurement can be performed.
The distance between the centre of the antenna array and the wind turbine is between 1000 m and 1200 m, this is a compromise between sensitivity and number of voxels (volume elements or volume pixels) available to image the wind turbine. There is no need to be exact because the system will be calibrated. It is important to place all antennas level and if possible also level with the wind turbine under test. The ITRS (International Terrestrial Reference System) coordinates of each antenna must be measured by competent land surveyors with an accuracy better than 6 cm RMS in all three dimensions.

Place the test source at 100 m height near or on the wind turbine, the test source is a comb generator that generates a signal with an e.i.r.p of $2.8*10^{-12}$W/Hz for each carrier. Discrete carriers are used to easily distinguish from interferers that might be present in the same frequency band. This is the 0dB reference level from the covenant and the system should always be able to detect this. This means that the power of the test source depends on the observation bandwidth of the instrument. Useful choices are the fine channel bandwidth of approximately 1 kHz, yielding $2.8*10^{-9}$W e.i.r.p., or the analysis band width of 1 MHz, yielding $2.8*10^{-6}$ W e.i.r.p. per carrier.

- First observation: test source off, wind turbine off
This observation is intended to perform a registration of possible interfering sources nearby and to set a low level reference value for the calibration procedure
The integration time is 1000 seconds in a 1 MHz observation bandwidth for a measurement aiming for -35 or -40 dB, 1800 s for a measurement aiming at -45 dB, and 7200 s for a measurement aiming at detecting the -50 dB level at a signal to noise ratio of at least 10.

- Second observation: test source intermitting 2 sec on/ 10 sec off wind turbine off
This observation is intended to establish the amount of reflected interference. The integration time is the same as before in a 1MHz observation bandwidth.

- Third observation: test source intermitting 2 sec on/ 10 sec off and wind turbine on. This is the actual measurement. The integration time is the same as before in a 1MHz observation bandwidth.

During the observation all IQ data for each receiver are collected and stored. A quick analysis should be performed on the data to see if the calibration source is visible. If not possible faults in the equipment should be corrected and the

measurement should be repeated. Rudimentary imaging may also be performed to identify potential local EMI unrelated to the wind turbine, so it can be dealt with before the main observation.

Process the data offline following the method described in section 4 and 5. Analysis will be done in a sequence of observation bandwidths of 1 MHz wide starting at 30 MHz up to 240 MHz, in this bandwidth both the mean wind turbine emission and its RMS fluctuations may not exceed the flux density levels corresponding to the -35dB or -50dB levels agreed upon in the covenant.

4 Digital pre-processing

This section describes the analysis of the data collected as described in section 5. The analysis method is described with code snippets forming a reference implementation in order to make it easier for a designer or data analyst to develop its own analysis software. The software suite from which the reference implementations were adapted is publicly available at https://github.com/brentjens/software-correlator.

The primary data consists of complex voltage (I/Q) data from every single antenna. The bandwidth per data stream could be anything from 1 MHz to the full 210 MHz. The received power per antenna due to the wind turbine is (much) lower than the power received from the brightest astronomical sources.
In addition to that, measurements are likely to be carried out in an environment where other sources of interference might exist.
Although one could attempt to beam-form the array by compensating the streams for geometrical delays and adding them, the resulting sensitivity towards the turbine will ultimately be limited by the accuracy of subtraction of astronomical sources from the data. Furthermore, beam forming towards a single direction precludes proper identification of the arrival direction of other, unrelated, interference.
A cross-correlating interferometer can be used to create images of the field of view of an antenna by using the van Cittert-Zernike theorem. These images show the radio flux density as a function of direction, thereby allowing one to positively identify the source of a certain signal, be it the wind turbine, an astronomical object, or other terrestrial interference. Following are the main steps involved in this process.

4.1 Antenna time series pre-processing

The I/Q data from an individual antenna is initially likely rather wide band, potentially several, if not tens of MHz wide. The van Cittert-Zernike theorem only holds for quasi-monochromatic radiation, hence the data must be channelized further. Because other interference in the 10-240 MHz band is mostly narrow band, going to of the order 1 kHz channel band width allows efficient removal of affected data to obtain a more reliable measurement of faint radio radiation from the wind turbine under test and astronomical sources.

When the required number of channels is large (which is likely to be the case here), it is more efficient to execute the subsequent cross-correlation of the antenna's time series by multiplication in the Fourier domain, hence the channelization must be performed before the cross correlation.

To prevent leakage of power between channels, we recommend to perform the channelization using a polyphase filter bank (PFB). A well designed PFB can provide more than 40dB isolation between neighbouring channels, and more than 100dB between all others. Source code in the Python language is provided in Reference implementation 4.1.

If the antenna/receiver band pass affecting the wide band I/Q data is known, this would also be a good place to divide the data by it to provide well-behaved antenna

data to the actual cross correlator. The act of channelizing does not change the data volume.

```
import numpy
import scipy.fftpack as fft
import scipy.signal as signal

def fir_filter_coefficients(num_chan, num_taps, cal_factor=1./50.0):
    raw_coefficients = signal.firwin((num_taps)*num_chan, 1/(num_chan),
                                     width=0.5/(num_chan))
    auto_fftshift = raw_coefficients*(-1)**numpy.arange(num_taps*num_chan)
    coefficients = numpy.array(auto_fftshift*(num_chan**0.5),
                               dtype=numpy.float32)
    coefficients *= cal_factor
    return coefficients.reshape((num_taps, num_chan))

def channelize_ppf(timeseries_taps, fir_coefficients):
    return (fft.fft((timeseries_taps*fir_coefficients).sum(axis=0)))

def channelize_ppf_contiguous_block(timeseries_taps, fir_coefficients):
    num_taps, num_chan = fir_coefficients.shape
    num_ts_blocks = timeseries_taps.shape[0]
    num_spectra = num_ts_blocks -(num_taps-1)
    output_spectra = numpy.zeros((num_spectra, num_chan),
                                 dtype=numpy.complex64)
    for sp in range(num_spectra):
        output_spectra[sp,:] += channelize_ppf(
                                    timeseries_taps[sp:sp+num_taps,:],
                                    fir_coefficients)
    return output_spectra


num_chan = 128
num_taps = 16
fir_coefficients = fir_filter_coefficients(num_chan=num_chan,
                                           num_taps=num_taps)
result = numpy.array([channelize_ppf_contiguous_block(
                          time_series_complex.reshape((-1, num_chan)),
                          fir_coefficients)
                      for sb in range(num_sb)],
                     dtype=numpy.complex64)
```

Reference Implementation 4.1: Python source code that applies a poly phase filter bank to complex valued time series data from a single antenna

4.2 Cross correlation

Once the antenna's time series are transformed to the frequency domain, cross correlations can be performed by multiplication of the complex spectrum of one antenna with the complex conjugate of another.
The result can be averaged in time for a period in which the interferometer's radio environment remains constant. This cross-multiplication has to be done for all possible pairs of antennas. Each pair of antennas is called a baseline, and provides a complex visibility representing one Fourier mode of the radio image one wants to create. To enable efficient removal of burst-like interference such as electric fences or lightning, we recommend averaging the data to approximately 0.1 s. Reference implementation 4.2 shows source code that implements cross-multiplication and averaging.

```
def cross_correlate_and_average(antenna_data):
    '''
    takes station dynamic complex spectra from one integration period, and
    computes the average cross correlation matrix.

    station_data : numpy array
                   Dimensions [station, time, frequency]
                   Values: complex64
                   This data structure is the output of the channel
                   separation stage.
    '''
    num_stations, num_times, num_frequencies = antenna_data.shape
    visibilities = []
    ad = antenna_data
    for antenna1 in range(num_stations):
        for antenna2 in range(antenna1, num_stations):
            avg = (ad[antenna1]*ad[antenna2].conj()).mean(axis=0)
            visibilities.append({'ANTENNA1': antenna1,
                                 'ANTENNA2': antenna2,
                                 'DATA': avg})
    return visibilities
```

Reference Implementation 4.2: Cross-correlation by multiplication of antenna data after having been transformed to the frequency domain.

The amount of output data per integration time is equal to B×C×w bytes, where B is the number of baselines including autocorrelations N×(N + 1)/2, with N the number of antennas, C the number of frequency channels, and w the width of the complex number. We recommend using complex numbers consisting of two four-byte floating point numbers. For 48 antennas and a 10 MHz total bandwidth divided into 5000 channels, this becomes approximately 47 MB per integration time of 0.1 s, or 470 MB per second of time on the sky. This is not necessarily the output data rate of the correlator because it does not have to run in real time, and might be implemented off-line.

4.3 Flagging and averaging

The high time- and frequency resolution data produced by the correlator still contains powerful narrowband interference from ordinary radio transmitters, as well as potential burst-like interference from, for example, electric fences. There also might be missing data due to various instrument malfunctions. Before averaging further, the affected data points must be marked ("flagged") as bad, so they can be ignored in the subsequent averaging, calibration, and imaging/-analysis stages. The most powerful algorithm currently in use at LOFAR for this task is based on the SumThreshold algorithm (André Offringa's PhD thesis) [8]. It simply adds sub sequences within an array (list of numbers in this case), and marks the subsequence as bad if the sum exceeds a certain threshold. The algorithm needs to be run in time direction for all channels, and in frequency direction for all time slots. Each baseline must be processed independently because some interference (for example generated by local equipment) might only show up on certain baselines. Before applying the SumThreshold algorithm, the data must be preconditioned by subtracting the mean and dividing by the root mean square (RMS) value. For sufficiently long observations or steep band passes, de-trending in time, frequency, or both might be necessary. After flagging, the data is recommended to be averaged to a resolution of approximately 1 s in time, and tens of kHz (depending on the interferometer up to 200 kHz is recommended) in frequency. This reduces the data size by a factor 100 to 1000. Subsequent steps are all conducted on the flagged and averaged data products.

```
def sum_threshold_2d(dynamic_spectrum, mask, threshold_sigma,
                     window_lengths=[1, 2, 4, 8, 16, 32],
                     threshold_shrink_power=0.45):
    num_times = dynamic_spectrum.shape[0]
    num_freqs = dynamic_spectrum.shape[1]
    window_lengths_time = [wl for wl in window_lengths if wl < num_times]
    window_lengths_freq = [wl for wl in window_lengths if wl < num_freqs]
    by_time_mask = sum_threshold_cython_2d(
        dynamic_spectrum.T.copy(), mask.T.copy(),
        threshold_sigma,
        window_lengths_time,
        threshold_shrink_power=threshold_shrink_power).T.copy()
    by_frequency_mask = sum_threshold_cython_2d(
        dynamic_spectrum, by_time_mask,
        threshold_sigma,
        window_lengths_freq,
        threshold_shrink_power=threshold_shrink_power)
    return by_frequency_mask


# Begin of main routine
flag_window_lengths =  2**numpy.arange(
    int(numpy.ceil(numpy.log(num_timeslots_in)/numpy.log(2))))
flagging_threshold = 5.0 # sigma
block_index = 0
baselines_per_chunk = 100
while True:
    buffer, baselines_read = input_h5.get_baseline_blocks(
                             block_index*baselines_per_chunk,
                             baselines_per_chunk)
    for bl in range(baselines_read):
        frame_data = numpy.abs(buffer.data[:, bl, :])
        frame_data -= frame_data.mean()
        data_std = frame_data.std()
        if data_std != 0.0:
            frame_data /= frame_data.std()
        flags = sum_threshold_2d(frame_data,
                                 buffer.mask[:, bl, :],
                                 flagging_threshold,
                                 window_lengths=flag_window_lengths)
        buffer.mask[:, bl, :] = flags
    block_index += 1
    if baselines_read < baselines_per_chunk:
        break
```

Reference Implementation 4.3: Preconditioning the data for flagging and executing SumThreshold in time- and frequency direction. The actual SumThreshold algorithm is not listed. Pseudocode can be found in Offringa's PhD thesis.

5 Imaging

5.1 Data model

There are several challenges that make detecting a wind turbine different from regular imaging. First, the expected signal is faint. Fainter in fact than the brightest few astronomical sources, Cassiopeia A (a supernova remnant), Cygnus A (a powerful radio galaxy), and the Sun. Second, although the astronomical sources are definitely in the interferometric far field, the wind turbine might not be. Furthermore, the wind turbine is so close that emission from different parts of the wind turbine may cause bright and dark interference patterns on the ground, leading to potentially large variations in the apparent brightness on different baselines. In the ideal, noiseless case, the cross correlation product of two antennas i and j at some quasi-monochromatic frequency υ due to K point-like sources at infinite distance.

$$V_{ij} = \sum_{k=1}^{K} I_k \mathrm{e}^{2\pi \mathrm{i} \nu (\vec{u}_{ij} \cdot \vec{l}_k)/c}$$

Where $\acute{u}$ is the difference vector $\acute{x_j} - \acute{x_\iota}$, and $\acute{l_k}$ is the unit vector pointing towards the source. $\acute{u}$ is colloquially called the "baseline".
$(\acute{u_{ij}}.\acute{l_k} \quad /c$ is the geometrical delay between the signal arriving at antenna i and antenna j . This equation is a discrete Fourier transform (DFT) between the "uv-plane" (coordinates $\acute{u}$) and the sky plane ($\acute{l}$).
For nearby sources, the expression becomes more complicated:

$$V_{ij} = \sum_{s=1}^{S} \sqrt{I_{si} I_{sj}} \mathrm{e}^{2\pi \mathrm{i} \nu (\|\vec{r}_{sj}\| - \|\vec{r}_{si}\|)/c}$$

where $\acute{r}_{si}$ is the vector $\acute{x_\iota} - \acute{x_s}$, and $I_{si}$is the apparent flux density of source *s* at the location of antenna *i*. Combining these, assuming one nearby source *s*, and adding cable delays per antenna, we have,

$$V_{ij} = g_i g_j \mathrm{e}^{2\pi \mathrm{i} \nu (\tau_j - \tau_i)} \left(\sqrt{I_{si} I_{sj}} \mathrm{e}^{2\pi \mathrm{i} \nu (\|\vec{r}_{sj}\| - \|\vec{r}_{si}\|)/c} + \sum_{k=1}^{K} I_k \mathrm{e}^{2\pi \mathrm{i} \nu (\vec{u}_{ij} \cdot \vec{l}_k)/c} + \sigma_{ij} \right)$$

where τ_i is the cable- and electronics delay for antenna i, g_i its signal path's voltage gain (antenna+electronics+cable), and σ_{ij} the Gaussian thermal noise on this baseline. Due to nearfield diffraction patterns, $I_{si} = I_s(1 + \sigma_{si})$ is expected to vary from antenna to antenna, and from frequency to frequency. It will depend on the details of ground conductivity, presence of scatterers close to the line of sight, and precise location of the transmitter and receiver. There are two realistic options to deal with this:

- Make images with the calibrator source on and off after subtracting the signal amplitudes of the astronomical sources, focused at the distance to the wind turbine, and compare the observed flux density at the location of the wind turbine with that of the calibrator source;

- Treat I_{si} as a Gaussian random variable with mean I_s and variance $\sigma^2{}_s$ and use Bayesian MCMC posterior sampling techniques to establish values and uncertainty contours.

Although the latter method is likely more informative, and gives a realistic estimate of the uncertainties involved, the former is easier to implement. During this project we have only been able to implement and test the first method.

5.2 Self-calibration

In radio imaging, one uses a technique called self-calibration, or selfcal to iteratively estimate the image of the sky and the complex gains $g_i e^{2\pi i \nu \tau_i}$ or in the quasi-chromatic approximation $g_i e^{i\phi_i}$, where ϕ_i is the phase and g_i the voltage gain of antenna i. The procedure is as follows:

1. Take flagged and averaged visibilities;
2. Using source positions from a source model, estimate source flux densities;
3. Using full source model (positions and estimated fluxes), predict "perfect" visibilities for all baselines;
4. Using "perfect" model visibilities and observed visibilities, determine complex antenna gains that minimize the difference between model and observed data;
5. Correct raw visibilities for complex antenna gains;
6. Subtract sources from corrected visibilities, make image, look for and identify new sources, add to sky model if found;
7. Using source positions from the updated source model and newly derived complex antenna gains, estimate brightness for each source;
8. Repeat from 3 until convergence is reached and the antenna phase solutions as well as the source flux densities stop changing.

This procedure converges in only a few iterations, provided that there are many more visibilities (equations) than the sum of the number of sources and the number of antenna gain solutions (unknowns), the signal-to-noise ratio per gain solution is sufficiently high, and the sky model contains almost all detectable sources.

Selfcal is very stable if one only fits for the antenna's phases and source fluxes. If one also attempts to solve for antenna gains, one requires a near-complete model of the sky to prevent unphysical solutions or diverging iterations. Generally, in radio astronomy, one starts out with several iterations of phase-only selfcal, followed by a few combined amplitude and phase iterations only when one is absolutely certain to have captured near 100% of the observed flux in the model. Given the small number of antennas and visibilities involved in the problem at hand, and the stability of analogue electronics at the relevant radio frequencies, we strongly advise against using amplitude selfcal and strongly recommend a phase-only approach.

The following subsections discuss the primary elements of the selfcal loop, the imaging, the calibration, and the source model or sky model.

5.3 Imaging

The main aim is to determine the apparent flux density (averaged over the array) of a source near the array, in the presence of several celestial sources at practically infinite distance. In the absence of a near-field source, one can form an approximate image of the sky by Fourier transforming the complex visibilities (array correlation matrix). If the antenna locations are fixed with respect to the area to be imaged, as is the case here, this is efficiently done by multiplying the vector of visibilities by a matrix M relating every pixel in the sky with every visibility. The

matrix M has as many columns as there are visibilities, and as many rows as there are pixels on the sky. Element m_{pq} of M is given by:

$$m_{pq} = w_q e^{2\pi i v(\vec{u}_q \cdot \vec{l}_p)/c}$$

where w_q is the weight of a certain baseline, $\vec{u}_g$ is the position difference vector pointing from antenna 1 to antenna 2 (which has its signals conjugated in the correlator) in the baseline, and $\vec{l}_p$ is the unit vector pointing to a certain pixel on the sky. Code to generate such a matrix is provided in Reference implementation 5.1.

The vector $\vec{w}$ could for example be 0 in case a certain visibility is not to be used, and *1/n* in case a certain visibility is one of *n* actually valid visibilities. Reasons to exclude visibilities could be that the baseline is too short, or the baseline contains other noticeable interference. The actual imaging is conducted as is shown in Reference implementation 5.2.

```
def make_imaging_matrix(uvw_m, freq_hz, l_rad, m_rad,
                        min_baseline_lambda=None,
                        max_baseline_lambda=None):
    arg     = 2j*numpy.pi*freq_hz/299792458.0

    u_m     = numpy.array(uvw_m[:, 0], dtype=numpy.float32)
    v_m     = numpy.array(uvw_m[:, 1], dtype=numpy.float32)
    w_m     = numpy.array(uvw_m[:, 2], dtype=numpy.float32)


    grid_l, grid_m = numpy.meshgrid(l_rad, m_rad)
    grid_l = numpy.array(grid_l.ravel(), dtype=numpy.float32)[:, numpy.newaxis]
    grid_m = numpy.array(grid_m.ravel(), dtype=numpy.float32)[:, numpy.newaxis]
    grid_n = nupy.sqrt(1 - grid_l**2 - grid_m**2)

    mat     = numpy.exp(arg*(u_m[numpy.newaxis, :]*grid_l \
                           + v_m[numpy.newaxis, :]*grid_m \
                           + w_m[numpy.newaxis, :]*grid_n))

    uv_lambda = numpy.sqrt(u_m**2 + v_m**2)*freq_hz/299792458.0
    bl_mask = numpy.ones(u_m.shape[0], dtype=numpy.int)
    if min_baseline_lambda is not None:
        bl_mask *= uv_lambda >= min_baseline_lambda
    if max_baseline_lambda is not None:
        bl_mask *= uv_lambda <= max_baseline_lambda

    return (mat.reshape((len(l_rad)*len(m_rad), len(uvw_m)))*bl_mask[numpy.newaxis,:],
            grid_l, grid_m)
```

Reference Implementation 5.1: Calculating a matrix to implement DFT imaging

```
def dft_image(matrix, num_pixels, acm_vector, weights=None):
    n = num_pixels
    if weights is not None:
        matrix_weights = numpy.abs(matrix).mean(axis=0)
        w = weights*matrix_weights
        wsum = w.sum()
        wlen = len(w)
        mat = matrix*w[numpy.newaxis,:]*wlen/wsum
    else:
        mat = matrix
    return numpy.dot(mat, acm_vector).real.reshape((n, n))
```

Reference Implementation 5.2: Calculating a matrix to forward-model visibilities due to sources at infinite distance.

The resulting all-sky image is shown in Fig. 5.1. The result of using a simple discrete Fourier transform for imaging is that one obtains a so-called "dirty" image, which is the true sky brightness distribution convolved with a point spread function (PSF). The PSF is obtained by Fourier transforming the weights between the baseline plane and the sky plane. Although the sources "Cas A", "Cyg A", "DR 4", "Tau A", and the Sun are clearly detected, all other blobs are side lobes of the PSFs centred on the brightest sources.

These side lobes dominate the noise floor of the map. To achieve map noise consistent with thermal noise, one has to remove these sources and their associated PSF side lobes. This deconvolution process is called "cleaning" in the radio astronomy world. There exists a vast literature describing the best algorithms for various situations.

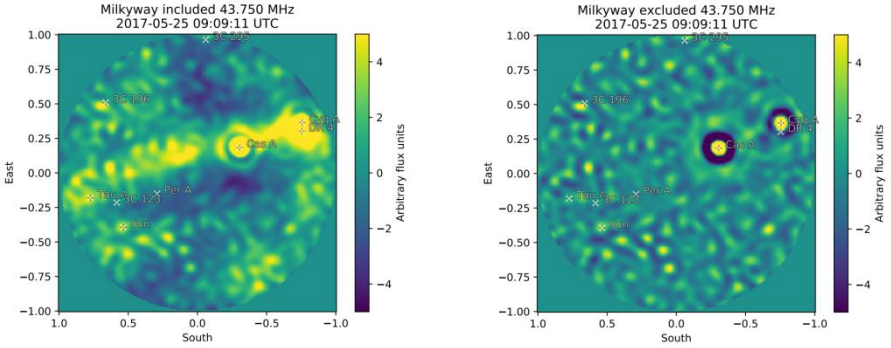

Figure 5.1: Image of the entire radio sky above LOFAR station CS302 at 43.750 MHz, obtained by directly Fourier transforming the visibilities. The brightest astronomical sources have been marked with crosses. The bright band from "Cyg A" via "Cas A" towards the eastern horizon is the Milky Way. The left image includes all baselines, while the right image only includes baselines longer than 4 wavelengths, effectively high-pass filtering the map to remove the diffuse Galactic radiation.

Because of the low number of sources that needs to be subtracted, and the small number of baselines, we choose to rewrite the first equation in section 6.4 in matrix form:

$$\vec{v} = M\vec{b}$$

where $\vec{v}$ is the vector containing all visibilities (obtained for example by taking the upper triangle of the array correlation matrix and stacking the rows or columns), $\vec{b}$ is the vector containing the (unknown) brightness of each source, and M is the matrix:

$$m_{pq} = w_p e^{2\pi i \nu (\vec{u}_p \cdot \vec{l}_q)/c}$$

With $\vec{l}_q$ the unit vector pointing towards astronomical source q. A routine to compute this matrix is listed in reference implementation 5.3.

```
def make_predict_matrix(uvw_m, freq_hz, source_lmn_rad,
                        min_baseline_lambda=None,
                        max_baseline_lambda=None):
    arg     = -2j*numpy.pi*freq_hz/299792458.0
    u_m     = numpy.array(uvw_m[:, 0], dtype=numpy.float32)
    v_m     = numpy.array(uvw_m[:, 1], dtype=numpy.float32)
    w_m     = numpy.array(uvw_m[:, 2], dtype=numpy.float32)
    source_l = numpy.array(source_lmn_rad[:,0], dtype=numpy.float32)[numpy.newaxis,:]
    source_m = numpy.array(source_lmn_rad[:,1], dtype=numpy.float32)[numpy.newaxis,:]
    source_n = numpy.array(source_lmn_rad[:,2], dtype=numpy.float32)[numpy.newaxis,:]
    mat     = numpy.exp(arg*(   u_m[:, numpy.newaxis]*source_l \
                              + v_m[:, numpy.newaxis]*source_m \
                              + w_m[:, numpy.newaxis]*source_n))
    uv_lambda = numpy.sqrt(u_m**2 + v_m**2)*freq_hz/299792458.0
    bl_mask = numpy.ones(u_m.shape[0], dtype=numpy.int)
    if min_baseline_lambda is not None:
        bl_mask *= uv_lambda >= min_baseline_lambda
    if max_baseline_lambda is not None:
        bl_mask *= uv_lambda <= max_baseline_lambda
    return mat*bl_mask[:, numpy.newaxis]
```

Reference Implementation 5.3: Calculating a matrix to forward-model visibilities due to sources at infinite distance.

One can then use any complex linear least squares solver to solve for the source fluxes. One can subsequently "predict" model visibilities by multiplying the solution vector $\vec{b}$ by the matrix M, and subtract these sources from the data. Re-imaging using the DFT imager will then allow one to search for fainter sources that may become visible once the bright sources and their PSF side lobes have been subtracted, so they can be added to the model. This process is illustrated in Fig. 5.2.

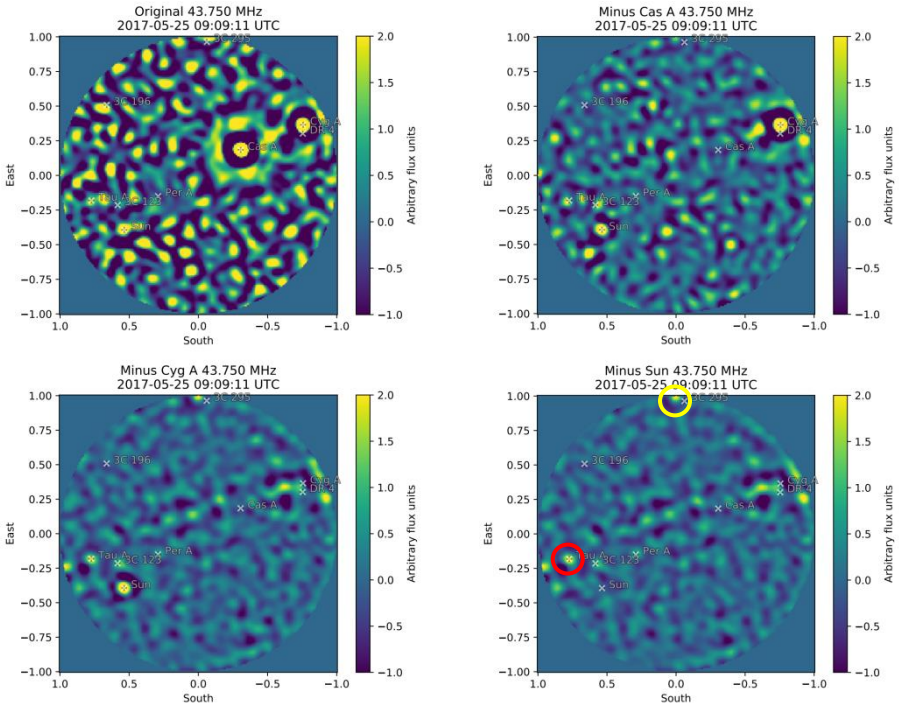

Figure 5.2: De convolving bright sources and their side lobes from the data.

At the end of this figure, Tau A is the brightest remaining source (red circle). Its side lobes, those of the complicated Cygnus-X region of the Milky Way at (-0.5,

+0.3), as well as those of a vacation park on the west-north-western horizon still dominate the noise level, so in practice one has to continue this process until no new sources are found. The test signal is already visible in the graph (yellow circle). The matrix form introduced before also applies to the case where sources are nearby. The only thing that changes is the phase structure of the column relevant to source in the interferometric near field. For nearby sources, the incoming wave fronts are spherical instead of planar:

$$m_{pq} = w_p e^{-2\pi i \nu (\|\vec{r}_{2pq}\| - \|\vec{r}_{1pq}\|)/c}$$

where $\vec{r}_{1pq}$ is the vector from baseline p's antenna 1 to source q. Code example 5.4 shows subroutines that compute this matrix for a set of nearby sources. The columns of this matrix can simply be appended to the matrix for the astronomical sources to jointly solve for astronomical and nearby sources. Note that the result for the nearby source is its mean apparent flux density at the mean position of the array, not the EIRP of the source itself. The latter can nevertheless be deduced from the solution by comparing it with the apparent flux density of the calibrator source.

```
def near_field_distances(pqr_ant, pqr_pixels):
    return numpy.array(numpy.linalg.norm(pqr_ant[:, numpy.newaxis, :]
                                         - pqr_pixels[numpy.newaxis, :, :], axis=-1),
                       dtype=numpy.float32)


def predict_matrix_near_field(ant_pqr_m,
                              freq_hz,
                              source_pqr_m,
                              phase_only=True,
                              min_baseline_lambda=None,
                              max_baseline_lambda=None):
    pqr_ant_m = numpy.array(ant_pqr_m, dtype=numpy.float32)
    distances_pqr = near_field_distances(pqr_ant_m, source_pqr_m)
    ant_gains = numpy.array(
        numpy.exp(-2j*numpy.pi*freq_hz*distances_pqr/299792458.0),
        dtype=numpy.complex64)
    if not phase_only:
        ant_gains /= distances_pqr
    baseline_gains = ant_gains[:, numpy.newaxis, :]*numpy.conj(ant_gains[numpy.newaxis, :, :])
    num_ant = ant_pqr_m.shape[0]
    matrix_rows = []
    uvw_m = acm_as_vector(baseline_matrix_m(ant_pqr_m), include_diag=True)
    for row_id in range(num_ant):
        for col_id in range(row_id, num_ant):
            matrix_rows.append(baseline_gains[row_id, col_id, :])
    mat = numpy.array(matrix_rows, dtype=numpy.complex64)
    uv_lambda = numpy.sqrt(uvw_m[:,0]**2 + uvw_m[:,1]**2)*freq_hz/299792458.0
    bl_mask = numpy.ones(uvw_m.shape[0], dtype=numpy.int)
    if min_baseline_lambda is not None:
        bl_mask *= uv_lambda >= min_baseline_lambda
    if max_baseline_lambda is not None:
        bl_mask *= uv_lambda <= max_baseline_lambda
    return mat*bl_mask[:, numpy.newaxis]
```

Reference Implementation 5.4: Calculating a matrix to forward-model visibilities due to compact sources at finite distance.

If the curvature of the wave fronts from a nearby source is not properly taken into account, and one simply assumes that the wave fronts will be planar like the ones from celestial sources, one will underestimate the flux density of the source. Figure 5.3 nicely illustrates this point with data and calculations for the case of the validation observations conducted at LOFAR station CS302.
If the wind turbine is sufficiently nearby that it subtends more than one PSF FWHM across the horizon (λ/D, where λ is the wavelength, and D the array's diameter), one might need to define multiple nearby "sources" (also known as "voxels" or "volume elements", analogous to "pixels" in 2D) covering the entire are of the wind turbine at Nyquist sampled direction intervals, and add the fluxes in all of them to obtain the total emission of the wind turbine under test.

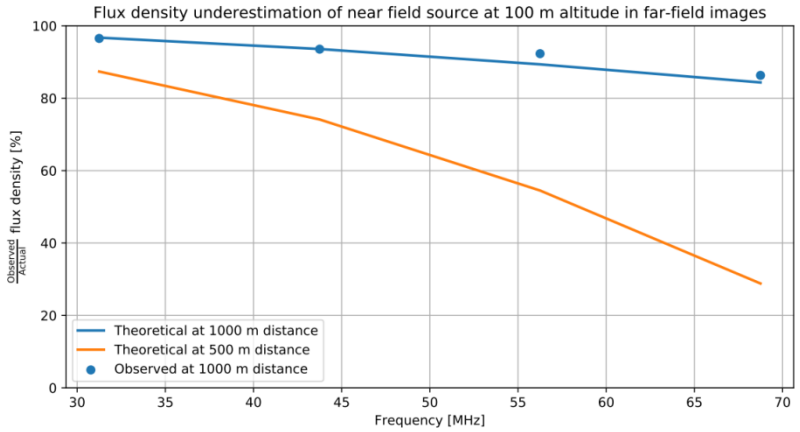

Figure 5.3: Underestimation of flux density of near field sources in far field images. Example using calculations for LOFAR station CS302 in the LBA OUTER configuration, showing data obtained during the May 2017 measurement method validation campaign

5.4 Calibration

The routine listed in Reference implementation 5.5 iteratively improves complex gain solutions per antenna, by minimizing the difference between the observed visibilities and model
visibilities generated by applying the combined far- and near-field measurement matrices to the derived fluxes, distorted by the complex gain solutions. The procedure itself is described clearly by various authors, for example Cornwell & Wilkinson (1981) [11], or Bhatnagar (2013)[12]. We recommend to only calibrate phases, and use all sources with apparent flux densities above the noise level of an individual solution interval in the sky model. Instead of solving for antenna gain amplitudes, or solving for ionospheric parameters per radio source, we have found that alternately solving for antenna gains, and source flux densities at time scales between 1 and 5 seconds, depending on ionospheric conditions, works quite well. This approach uses S + N degrees of freedom for S sources (celestial or nearby) and N antennas, out of order N(N - 1)/2 equations (the visibilities). In practice, there are a little less visibilities if certain data were discarded due to other interference or the baseline being shorter than 4 wavelengths. Donoho & Tanner (2009)[13] derive the precise conditions under which similar estimation problems do and do not converge. As a rule of thumb one should make sure that S + N is (much) smaller than half the number of useful baselines.

```
def antsol(vis_data_vect, vis_model_vect,
                gain_solutions, antenna1_vect, antenna2_vect,
                baseline_weights, alpha=0.5, epsilon=1e-5, refant=0,
                max_iter=200):
    vis_mask = vis_model_vect == 0.0
    model = ma.array(vis_model_vect, mask=vis_mask)
    vis_pointsource = ma.array(vis_data_vect/model, mask=vis_mask)
    num_ant = len(gain_solutions)
    w = baseline_weights
    x_mat = numpy.zeros((num_ant, num_ant ), dtype=numpy.complex64)
    w_mat = numpy.zeros((num_ant, num_ant ), dtype=numpy.float32)
    ant1 = antenna1_vect
    ant2 = antenna2_vect
    for a1, a2, v, w in zip(ant1, ant2, vis_pointsource, w):
        x_mat[a1, a2] = v
        x_mat[a2, a1] = numpy.conj(v)
        w_mat[a1, a2] = w
        w_mat[a2, a1] = w
        if a1 == a2:
            w_mat[a1, a2] = 0

    g_prev = gain_solutions
    g_next = numpy.zeros((len(g_prev),), dtype=numpy.complex64)
    iteration=0
    mask = False
    while True:
        den = ma.array((w_mat*(numpy.abs(g_prev)**2)[numpy.newaxis, :]).sum(axis=1),
                       mask=mask)
        mask = den == 0.0
        den.mask = mask
        if mask.all():
            break
        num = ma.array((x_mat*w_mat*g_prev[numpy.newaxis,:]).sum(axis=1), mask=mask)
        g_next = g_prev + alpha*(num/den - g_prev)
        if norm(g_next-g_prev)/norm(g_next) < epsilon:
            break
        iteration += 1
        g_prev = g_next
        if iteration >= max_iter:
            mask = mask+True
            break
    return ma.array(g_next/exp(1.j*angle(g_next[refant])), mask=mask)
```

Reference Implementation 5.5: Algorithm to estimate complex gain solutions per antenna, given the observed visibilities and simulated model visibilities

5.5 Source model and coordinates

To estimate source flux densities from interferometric data, it is essential to know where the sources are supposed to be as seen from the interferometer. Although a wind turbine or calibration source are likely stationary, astronomical sources appear to move across the sky due to the Earth's rotation. The sky model's task is to calculate the apparent positions of sources so that the model matrices can be calculated with the correct phase differences per antenna pair. For each astronomical source, several coordinate conversions need to be performed. For the sun, one also needs to calculate the earth's position in the solar system. Fortunately there are several libraries written for expressly these purposes, for example "Standards of Fundamental Astronomy" (SOFA, http://www.iausofa.org/). A more generically useful Python library called "astropy" (http://www.astropy.org/) uses a clone of SOFA called "Essential Routines for Fundamental Astronomy" (ERFA, https://github.com/liberfa/erfa).

The interferometric imaging is done in a cartesian coordinate system on the sky with coordinates "l", "m", and "n". The origin of the system coincides with the centre of the array. "m" points north parallel to the plane of the array, "l" points east parallel to the plane of the array, and "n" points up, perpendicular

to the plane of the array. The ‟lmn" vector always has unit length. When talking about coordinates of the antennas or sources close to the array, we use a parallel coordinate system in units of meters, with ‟p" parallel to ‟l", ‟q" to ‟m", and ‟r" to ‟n". The baseline coordinates ‟u", ‟v", and ‟w" are calculated by subtracting the ‟pqr" coordinates of the antennas that form said baseline. In the case at hand, the ‟pqr" and ‟lmn" coordinates are therefore fixed with respect to the array, and therefore its specific location on our planet. One can therefore go from ITRS coordinates (International Terrestrial Reference System) to ‟pqr" / ‟lmn" by applying a constant origin shift and a constant rotation matrix.

Celestial source coordinates are generally listed or calculated in ICRS (International Celestial Reference System), which has its origin at the solar system barycentre. To take into account the effect of parallax (particularly for solar system bodies) and aberration due to the finite speed of light, the ICRS coordinates need to be transformed to GCRS (Geocentric Celestial Reference System).
From there one can convert to ITRS through application of the earth rotation and orientation parameters provided by the International Earth Rotation and Reference Systems Service (IERS).

The whole conversion path is therefore for every time slot in the visibility data set (i.e. roughly every 0.1 to 2 seconds!)

1. Calculate solar ephemeris in ICRS for date and time of observation
2. Convert to GCRS at ITRS location of the centre of the array
3. Convert to ITRS at date and time of the observation and location of the array
4. Apply fixed shift and rotation to go to ‟pqr" / ‟lmn" system.

Of course one should only use those sources that are above the horizon. if the array is level and in generally flat terrain, one can simply take all sources for which the ‟n" coordinate is larger than 0. In case of a mountainous environment, one should invest in the construction of a horizon model in the ‟lmn" system.

5.6 Final calculations in terms of covenant limits

To arrive at a proper amplitude calibration, one first needs to perform the analysis described in this chapter on the data containing the calibration source. Because of the interference patterns to be expected on the ground, it is advised to use a phase-only selfcal, and simultaneously fit for the flux density of the calibrator as well as the astronomical sources for each individual time slot. because this is on uncalibrated data, the units will be on an arbitrary flux density scale, which is the same for the calibrator data and the wind turbine data. To reflect this, this arbitrary flux scale is measured in "flux units".

One can now calculate the mean and standard deviation in the mean of the flux density (flux divided by bandwidth over which the data have been integrated) of the calibrator source in "flux units".

Subsequently, one applies the phase solutions that were obtained (averaged in time) to the wind turbine data, and repeat the self cal and source fitting on the data without the calibrator source. This gives the wind turbine flux density in "flux units". Depending on the size of the wind turbine, distance to the wind turbine, the size of the antenna array, and the observing frequency, it may be necessary to represent the wind turbine by several points in 3D space, called "voxels" (volume elements), and to add the flux density found in each of them to arrive at the total flux density of the wind turbine.

The final emission of the wind turbine in terms of the covenant, is then given by

$L = P_{cal} + 85.6 - 10 \log_{10}(B) + 10 \log_{10} (W \times D_w^2) - 10 \log_{10} (C \times D_c^2)$,

where L is the covenant level in dB, P_{cal} is the E.I.R.P of the (narrow band) calibrator signal in dBm, B is the band width used for the analysis in Hz, W is the flux density of the wind turbine in "flux units", D_w is the distance to the wind turbine in m, C is the observed flux density of the calibrator in "flux units", and D_c is the distance to the calibrator source. For the distances one should use the Euclidian distance between the mean position of the antennas and the centre of the voxel containing the wind turbine or calibrator source.

The value L must be determined for the observations with the wind turbine fully powered off, as well as fully powered on. The radiated level is then estimated by $L_{radiated} = 10 \log (10^{Lon/10} - 10^{Loff/10})$. We basically perform the calculation according to the previous formula twice, the subtraction lets us with the wind turbine emission only.

It is of course crucial that the observation with the wind turbine powered off is conducted as close in time as possible to the observation with the wind turbine running at full production capacity.

6 Design challenges

This section describes a number of design considerations for the measurement setup for separate measurement challenges to be solved: how to adequately determine the (equivalent) interference in the far field, attain the required sensitivity, and make enough discrimination from other interference sources at the same time.

6.1 Definition of the field strength to be measured

The field strength to be measured is defined in the covenant as follows.
(use the original Dutch text in case of legal purposes)

In Article 1
"The (equivalent of) the limit values in EMC norm EN55011 for class A group 1, of 50 dBµV/m in a bandwidth of 120 kHz (this is equivalent with – 0,8 dBµV/(m ⋅ Hz)) at 10 m distance of the wind turbine nacelle at 100m height, are used as reference for the agreement in this covenant ("Norm")."

In Article 2:
"The windfarm shall not be put in operation by the initiators if the EM interference of the wind turbines is not at least 35dB below the norm in the direction of the LOFAR core if the windfarm is in full operation.

In addition to that a -50dB value is defined for which the windfarm is not subject to operational limitations

The interpretation of this field strength can be found in the Interference Report [10]. The value is related to the value in an EMC norm however the value is not an EMC value in terms of measurement and can therefore not be measured using any EMC method. The measurements have to be performed as mean/RMS measurements because wind turbine interference to LOFAR's imaging observations is linearly proportional to the mean flux density of the wind turbine, and LOFAR's time domain observations are affected linearly proportionally to variations in the signals. The measurement bandwidth is chosen based on the victims observation bandwidth and maximum allowed data loss and set at 1 MHz. Additional information on this can be found in the Interference Report [10].

The field strength in the covenant is "victim" oriented, defined as the field strength at the LOFAR core generated by a point source at 100 m height.

The field strength is defined in the geometric far field. In case of a near field measurement, far field values have to be derived by calculations.
A few options to do that with their pros and cons are described in section 3.
It should be noted that for the higher frequencies, the far field starts at a very large distance from the radiator (wind turbine).

6.2 Conditions for measuring the field strength (far field condition)

The measurement of field strength is related to the definitions in section 6.1.
A wind turbine is an object with a largest dimension of more than 100 m. For the calculations in this section, a dimension of 100 m is used. The frequency range of interest is 30 MHz to 240 MHz. This makes it necessary to treat the wind turbine as a radiator in different ways depending on frequency ranges.

In the object with a dimension of 100 m, multiple EM sources are located, irregularly divided over the length of the structure.
For the higher frequencies the EM sources form an array and the behaviour of the elements of the array is unpredictable. The composition of the array is also not constant because of the rotating blades of the wind turbine.
For the lower frequencies the object behaves as a radiator with a length of several wavelengths and a varying dimension.

For determining the geometric far field for the higher frequencies the whole array needs to be taken into account. Normally we use the criterion of 10° phase difference between the elements of the array. As a consequence of this the far field starts at different distances for different frequencies. At the maximum frequency of 240 MHz where $\lambda = 1{,}25$m , the far field starts at 144 km when using the straight forward geometric calculation method below.

The calculation method is a simple geometric calculation based on the difference in path length between A (to the top of the wind turbine) and B (the measurement distance), as depicted in figure 6.1. This needs to be shorter than (λat 240MHz)/36, to fulfil the 10° phase difference criterion.

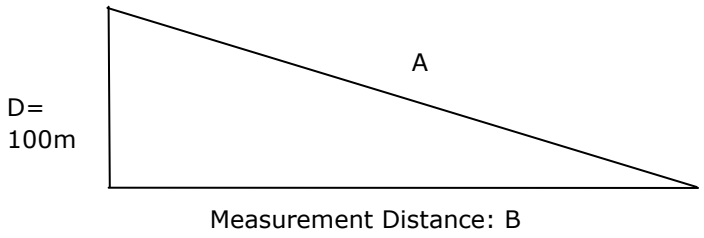

Fig 6.1 Height of radiator versus measurement distance

The path difference can be approximated by $(A-B) = D^2/2B$, under the condition that (A-B) is much smaller than D. So the measurement distance should be $B > D^2/2.(A-B)$, where (A-B)= λ/36 .

At the lower frequencies we consider the radiator not as an array but as a single radiator with a length of several wavelengths. It is then appropriate to use the formula for the Fraunhofer distance $d_{Fraunhofer} = \frac{2D^2}{\lambda}$,
where $d_{\text{Fraunhofer}}$ is the Fraunhofer distance in meters, D the largest dimension of the radiator in meters and λ the wavelength.

The transition between both approaches is not abrupt and we also need to include the dimensions of the victim and the distance to the interferer in this approach.
A number of solutions to measure field strength on a large radiator are possible.

Case1: For measurement situations where the far field condition cannot be achieved a near field scan needs to be performed were both amplitude and phase are measured at different points in the ares around the radiator. With these values the field strength at a certain point in the far field may be calculated.

Case 2: A method usually used in for example EMC measurements is to perform a height scan over a full wavelength in order to determine the maximum or average field strength, depending on the measurement type, at a certain point in the near field. This cannot be used for field strength measurements.

Case 3: A "true" field strength measurement is performed in the far field. To eliminate the effect of mainly ground reflections, a height or distance scan needs to be performed to be able to average out these reflections.

Table 6.1 gives an overview of different distances and frequencies where we have a far field condition in the case of an object with 100 m dimension.

Distance m	Freq far field 10° criterion [MHz]	Freq far field Fraunhofer criterion [MHz]
500	0.9	7,5
1000	1,6	15
2000	3,3	30
3000	5,2	45
4000	6,6	60
5000	8,3	75

Table 6.1 Far field distances vs frequency in the case of an object with 100 m dimension

6.2.1 Additional precautions to take into account when developing a measurement method

The field strength around the interferer basically manifests itself as a frequency dependent interference pattern of direct and reflected waves. The pattern is in motion because of the rotating blades of the wind turbine. This means that when developing a measurement method, this method needs to be able to cope with this effect when measuring at relatively short distances.

6.3 Sensitivity versus distance (field strength calculation)

This section provides a theoretical exercise to explain the challenges to obtain sufficient sensitivity when developing a measurement system. Calculations based on the -35dB level from the covenant are performed using a logperiodic antenna as an example antenna.

Field strength can be calculated using radiated power and distance to the source using the following formula:

$E = 5.48\frac{\sqrt{P}}{R}$ where E is the field strength in V/m, R the distance in meters and P the radiated power in W.

A field strength of – 0.8 dB(µV/m/Hz) at 10m distance equals an e.i.r.p of $2.8*10^{-12}$W/Hz, or $33.6*10^{-8}$ W in 120 kHz, or $2.8*10^{-6}$ W in 1 MHz.

Using the method from the Interference Report, we calculate everything back to a point source with a defined radiated power and position this at a height of 100 m. With this value we can plot a field strength vs distance curve.
The curve for free space is plotted in figure 6.2, this curve is used in further calculations. For clarity, the curve is split in two parts: one part for 0-100 m and one part for 100-5000 m. We use for e.i.r.p the value / Hz because we need this to determine the sensitivity of the receiving equipment. The reference distance and distances of 2000 m, 3000 m and 5000 m used later in this report are marked.

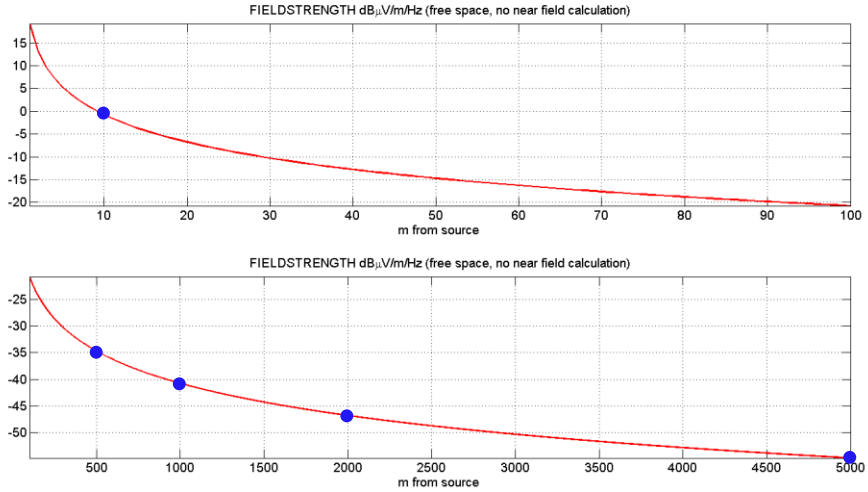

Fig 6.2 Field strength per unit bandwidth versus distance for an emission with an e.i.r.p. density of $2.8*10^{-12}$W/Hz. This corresponds with the reference level (norm) of – 0.8 dB(µV/m/Hz) at 10 m distance and 100 m height from the wind turbine. Free space propagation loss is assumed.

At a distance of 500m, 1000m, 2000 m, 3000 m and 5000 m, the field strength of our reference source is respectively -35dB(µV/m/Hz), -41dB(µV/m/Hz),-47dB(µV/m/Hz),-50dB(µV/m/Hz) and -55dB(µV/m/Hz).

Assuming a logarithmic periodic (logper or logperiodic) measurement antenna with a gain of 7dBi [5] we can translate these field strengths to a terminal voltage at the measurement receiver over 50 Ω using the following formula [1], $K=20\log f-G-29{,}78dB$.

K is a constant with unit dB(1/m), G is antenna gain in dBi, and f the frequency in MHz. Assuming a constant gain of the measurement antenna the terminal voltage is not constant but varies with the frequency.

In figure 6.3 the terminal voltage is converted to dBm/Hz for distances of 2000 m, 3000 m and 5000 m. An e.i.r.p. density of $2.8*10^{-12}$W/Hz measured using a receiver

bandwidth of 120 kHz bandwidth corresponds with an e.i.r.p of $3.4*10^{-7}$ W or -35 dBm.

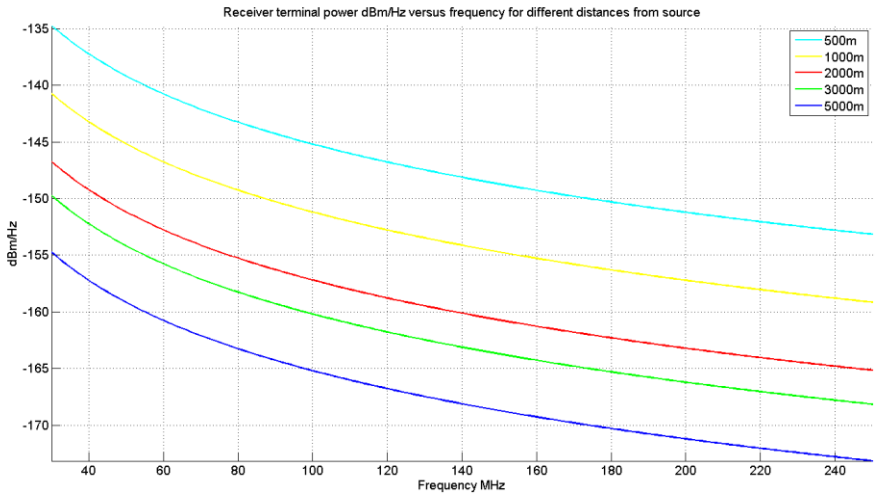

Fig 6.3 Power per unit bandwidth at the antenna output versus frequency for an emission with an e.i.r.p. density of $2.8*10^{-12}$W/Hz. This corresponds with the reference level (norm) of – 0.8 dB(µV/m/Hz) at 10 m distance and 100 m height from the wind turbine. Free space propagation loss is assumed. Five distances are shown: 500 m (cyan), 1000 m (yellow),2000 m (red), 3000 m (green) and 5000 m (blue).

To provide confidence during the measurements it is advisable to be able to measure below the lowest expected signal in order to see if in the case of a well-functioning low EMI wind turbine, the measurement equipment is still showing weak signals above the receiver noise floor. Taking into account measurement uncertainty and practical experience, 10dB is required as a minimum value for "headroom", but a higher value may be decided on by the developer of the measurement system. This results in minimal 45dB below the signal strength caused by the maximum calculated radiated power. The radiated power itself needs to be at least 35dB below the reference power in order not to cause interference as indicated in section 1. To perform a reliable noise measurement the signal to be measured needs to be at least 10dB above the receiver noise [2], [3], [4].
The advised headroom and level above the noise floor are two separate conditions that both need to be fulfilled.

This "headroom" and level above the noisefloor are not included in our calculation. Figure 6.4 shows the curves from figure 3 lowered by 35dB. An e.i.r.p. density of $8.9*10^{-16}$W/Hz measured using a receiver bandwidth of 120 kHz bandwidth corresponds with an e.i.r.p of $1.1*10^{-10}$ W or -70dBm.

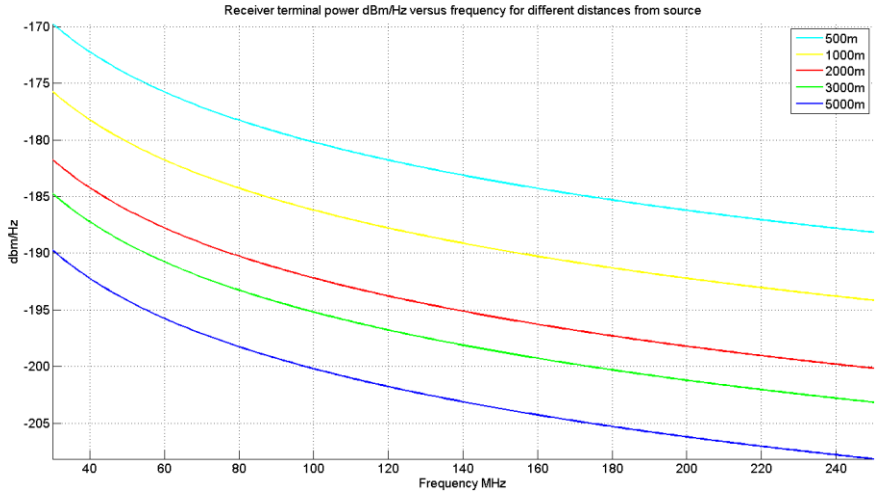

Fig 6.4 Power per unit bandwidth at the antenna output versus frequency for an emission with an e.i.r.p. density of $8.9*10^{-16}$W/Hz. This corresponds with the agreed level 35dB below the norm. Free space propagation is assumed. Five distances are shown: 500m (cyan),1000 m (yellow),2000 m (red), 3000 m (green), and 5000 m (blue).

NOTE: Especially at lower frequencies an antenna such as the log periodic antenna mentioned in this section exhibits a much lower gain than the 7dBi assumed in this section.

6.4 Insufficient sensitivity of a standard measurement approach with high end equipment

In table 6.2 a number of examples of high end measurement receivers / spectrum analysers are given indicating their maximum sensitivities.
The information in this table shows that, at a measurement distance of 1000 m, we are already more than 30dB below the required sensitivity.

	Frequentierange 10MHz - 200 MHz					
	Hi End analyzers			Property AT		
	R&S® **FSW** Signal and Spectrum Analyzer	Keysight **N9030B PXA Signal Analyzers**	Tektronix **RSA6106B**	R&S **FSV**	R&S **FSMR**	Tektronix RSA**306B**
Sensitivity dBm/Hz	-150dBm @1M-1G	-155dBm @1M-10M	-149@>10M-100M	-152dBm @1M-1G	-155dBm @20M-2G	-161dBm @5M-1G
IP3	>25dBm @10M-1G	+13dBm @10M-150M	13,5dBm	>12dBm @10M-100M	>17dBm @10m-300M	+13 dBm @2130M
measurement uncertainty	<0,2 dB	0,24dB	0,5dB	<0,2 dB	<0,2 dB	1,2 dB
Largest - Smallest IF filter	1Hz - 10MHz	1Hz - 8 MHz	0,1Hz-8MHz	1Hz-10MHz	10Hz-20MHz	10Hz - 8MHz
IQ output to matlab, labview of disk in a usable format	option	option	option	yes	yes	yes

Table 6.2 Sensitivity – i.e. minimum detectable power per unit bandwidth – of several high-end measurement receivers

Combining a well performing analyser, following the example of table 6.3, with a LNA having a gain of 23dB results in a 19dB SNR at 100 MHz and 1000 m when

measuring the reference signal level. Measuring 35dB below this level results in a SNR of -22dB. The reference level according the norm can therefore be measured, but the reference level -35dB cannot be measured in this situation. Cable attenuation is ignored in this example.

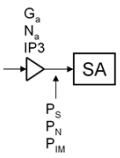		
Input power	-157	dBm
Gain of LNA	23	dB
Noise figure of LNA	1,2	dB
OIP3 of LNA	37	dBm
Resolution bandwidth of SA	1,00E-06	MHz
Input attenuation of SA	0	dB
DANL of SA	-150	dBm/Hz
IP3 of SA	13	dBm
Power on input SA	**-134**	**dBm**
Cascaded noise figure	4,1	dB
Noise floor	**-147**	**dBm**
Cascaded IP3	13	dBm
3rd order intermod	**-428**	**dBm**
SNIR	**13**	**dB**

Table 6.3 Calculation example sensitivity measurement receiver with LNA at 100 MHz and 2000 m distance

Conclusion: A single antenna with LNA and well performing spectrum analyser is not sufficient to check the emission level at 1000m distance.

6.5 Enough discrimination from other interferers

During a measurement not only the radiation from the wind turbine will be received but also interference from other manmade EMI sources and astronomical objects is present. This interference needs to be subtracted from the total received radiation. The antennas need to be placed in such a way that the used processing method is able to distinguish between far field interferers and near field wind turbine radiation.

7 Design Solution

The definitive measurement solution consists of an array of multiple receivers and antennas and a processing algorithm. The actual layout (size and baseline) and minimum number of antennas to measure the signals specified in the covenant is determined in this chapter. The same is valid for the processing algorithm which should produce an output using data from a reasonable data collection period.

In this section the unit Jansky (Jy) is used. This unit is named after pioneer radio astronomer Karl G Jansky and is the unit of flux density used in radio astronomy 1Jy= 10^{-26} W/m^2/Hz. The unit is of practical use in calculations where astronomical objects with known brightness are used since they are expressed in this unit. The sensitivity of LOFAR and other radio telescopes is also expressed in this unit. The exact relation of with the value from the covenant is discussed in annex E.

7.1 Calculated minimum configuration

A pre-analysis for a minimum configuration is made based on the starting point that a practical configuration should preferably not be larger than about 10 antennas. A measurement sensitivity of -35dB below – 0.8 dB(µV/m/Hz) over 120 kHz bandwidth at 10 m distance from the interferer should be achieved for the whole frequency range of 30-240 MHz. There should also be a 10dB headroom in order to prove that a signal is really below the maximum level allowed by the covenant. The data collection time is likely best kept below 2 hours to prevent changes in the measurement setup environment. A minimum of 1000 seconds is necessary to average over (and measure) short timescale fluctuations.

7.2 Sensitivity calculation

We first calculate the flux density of an emitter as a function of distance, assuming a direct line-of-sight between transmitter and receiver. We assume that the EMI is radiated isotopically, over 4π steradians.

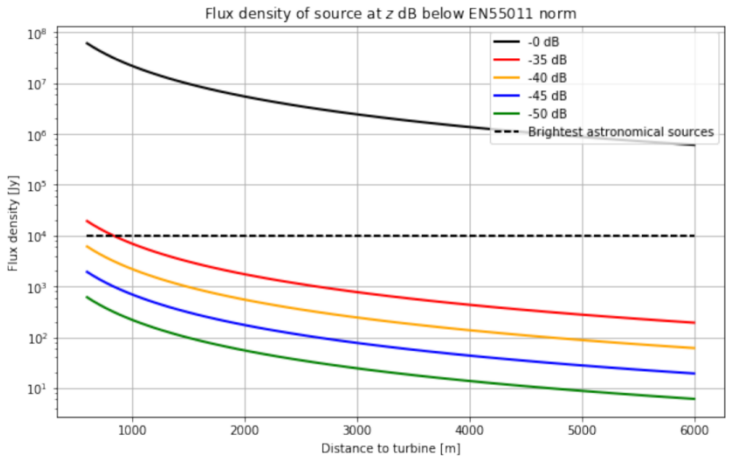

Fig 7.1 Field strength produced by source expressed as astronomical flux density vs distance

The expected flux densities depicted in figure 7.1, set the required sensitivities for the measurement apparatus. The power gain and effective area of an antenna are related via:

$$G = \frac{A_{eff} 4\pi}{\lambda^2}$$

See Kraus [6] for details.
Thomson, Moran, and Swenson [7] give the interferometric map noise for a single polarization as

$$S_{rms} = \frac{2kT}{A\sqrt{n_a(n_a - 1)\Delta v \Delta t}}$$

or in terms of the gain of an individual antenna:

$$S_{rms} = \frac{2kT4\pi}{G\lambda^2\sqrt{n_a(n_a - 1)\Delta v \Delta t}}$$

Assuming the noise temperature is dominated by Galactic noise, Rec. ITU-R-P.372 lists the following relevant expressions: Noise figure F_{am}=52-23 log f.
where f in MHz, brightness temperature $T_b = T_{b0}\frac{f^{-2.75}}{f_0} + 2.7K$, where T_{b0}=200 K at 408 MHz. We assume T_{b0}=40 K at 408 MHz since we prefer to do the observations when the Galactic centre is below the horizon, to minimize the noise temperatures of the antenna.

Relevant for measurement equipment is bandwidth. We require a 1 MHz analysis bandwidth. We need to estimate the number of antennas required to obtain an SNR of at least 10 dB within 1000 seconds of data.

Table 7.1 gives an overview of antennas with a gain between -12 and 2dBi towards the wind turbine under test and the minimum number of antennas needed to measure different levels and different observation/measurement times. It is clear that the number of antennas required for the most sensitive observations quickly becomes unwieldy when integrating for only 1000 seconds, unless an antenna design with significant gain towards the target is used. Although practical wide band with positive gain are fairly easy to come by above 70 MHz, most moderately wide band designs working at 30 MHz have rather poor gain towards the horizon.

Antenna dBi towards target	number of antennas -35 dB (1000 s)	number of antennas -40 dB (1000 s)	number of antennas -45 dB (1800 s)	number of antennas -45 dB (7200 s)	number of antennas -50 dB (1000 s)	number of antennas -50 dB (7200 s)
-12	20	63	148	74	626	234
-10	13	40	94	47	395	148
-8	8	25	59	30	250	93
-6	5	16	38	19	158	59
-4	4	10	24	12	100	37
-2	2	7	15	8	63	24
0	2	4	10	5	40	15
2	1	3	6	3	25	10

Table 7.1 Required # of antennas as function of absolute gain in dBi

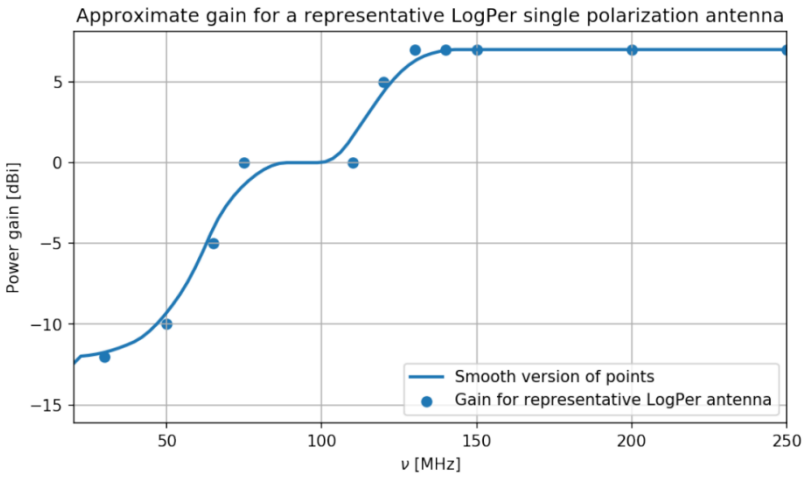

Fig 7.2 Assumed gain of a single antenna element vs frequency

Figure 7.2 shows a fairly representative gain curve for a log-periodic antenna. Assuming an antenna gain for an individual element as depicted in figure 7.2 we can calculate the total noise arriving at the receiver and in turn the sensitivity for one element can be calculated. The results are given in figure 7.3.

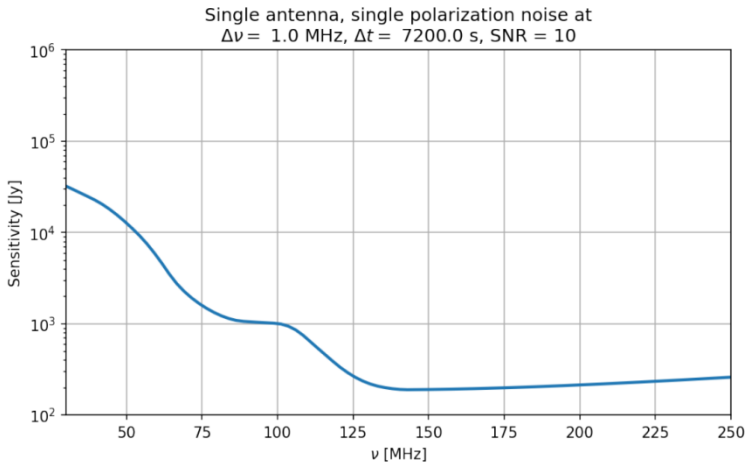

Fig 7.3 Single antenna element calculated sensitivity

With the data from the previous calculation, the total sensitivity of an array of antennas with a particular baseline can be calculated. This sensitivity also depends on integration time and distance to the interferer.

In figure 7.4 the number of needed antennas versus frequency and sensitivity is plotted for three different distances. This again assumes the log-per from figure 7.2. For the lowest frequency at 1472 m distance a minimum of 10 antennas is required to measure 35dB below the reference level at a signal to noise ratio of 10 dB, see the red curve.

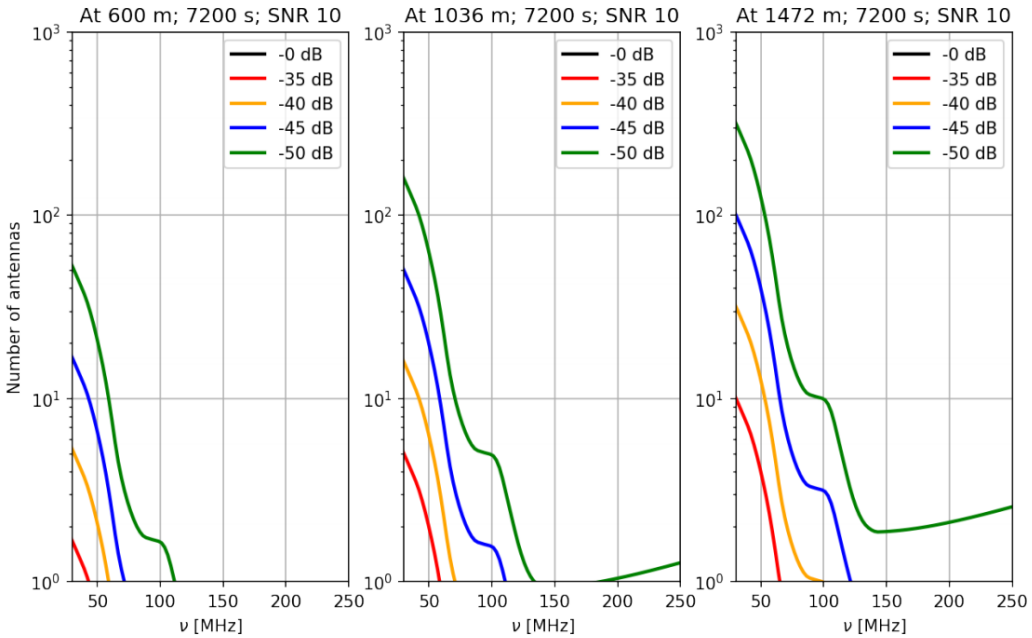

Fig 7.4 # of needed antennas versus frequency and sensitivity based on test logper antenna with specs in fig 7.2

7.3 Array configuration

The uncertainty with which a wind turbine's EMI can be determined has four main contributors:

- The uncertainty in the calibration source's transmitted e.i.r.p.
- Stochastic noise due to thermal noise in the antennas and receiver chain
- Side lobes from other radio sources falling on top of the wind turbine's location
- Errors in the subtraction of bright sources due to Point Spread Function (PSF) distortions caused by calibration errors.

Although the first item does not depend on the array's configuration and antenna design, the latter three items do, at least in part. In fact, they can be used to define minimum necessary array configurations. In the following treatment we will only discuss the second and third item.

Both the thermal noise, as well as the side lobe noise from radio sources that were not taken into account during the deconvolution / source subtraction step, manifest themselves as independent contributions to the RMS noise of a sky image after subtraction of the astronomical sources and the wind turbine (or calibration source). The thermal noise and side lobe noise are mutually uncorrelated, so their contributions add quadratically. We therefore aim for both of them to be at most $1/\sqrt{2}$ of the noise level that needs to be achieved for a signal-to-noise ratio of 10 on the relevant emission level from the covenant. A measurement of the -50 dB therefore requires a total image noise equivalent to the -60 dB level. Table 7.2 enumerates the required noise levels in units of Jy for the case of a source at 100 m height and 1000 m horizontal distance:

Covenant level [dB relative to ref level]	Flux density at 1000 m distance, 100 m height [Jy]	Required noise level [Jy]
0	21,714,400	2,171,4400
-35	6,875	688
-40	2,174	217
-50	217	22

Table 7.2 Required noise levels in units of Jy for the case of a source at 100 m height and 1000 m horizontal distance

Using a band width of 1 MHz and the equations from the previous sections, we can calculate the bare minimum number of antennas needed to achieve the required thermal noise level as a function of covenant level, antenna+receiver gain in dBi, and integration time. We have attempted to design for 1000 s integrations, but as is clear from Table 7.2, the more sensitive levels can only be reached with reasonable numbers of antennas if one integrates for up to two hours. Making the measurements last longer is likely not going to improve the quality of the measurement, because the environment might start to change too much. Think of wind speed and direction, precipitation, changes in atmospheric propagation conditions, etc.

The log periodic example antenna used in the previous sensitivity estimates has a gain of -12 dBi at 30 MHz, while a resonant, narrow band vertical monopole antenna specifically designed for 30 MHz might have a gain up to about +2 dBi. Reasonable, moderately wide band designs can likely perform at the -8 dBi level or better, which is what we assumed for the example configurations in this section. So, at -8 dBi gain towards the target, one needs at least 8 antennas for the -35 dB level, 25 for the -40 dB level, 30 for the -45 dB level (if one integrates for 1800 instead of 1000 seconds), and 93 for the -50 dB level (if one integrates for at least 2 hours). However, the PSF side lobes of not subtracted sources also lead to a minimum number of antennas. The RMS image noise due to a single source with flux density I, affected by the array's PSF, is:

$$\mathrm{RMS} = I \times \mathrm{RMS}_{PSF}$$

Assuming the locations of sources are uncorrelated with the PSF side lobes, we can determine the RMS noise due to not subtracted sources by quadratically adding their individual contributions:

$$\mathrm{RMS}^2 = \sum_{k=1}^{k} {I_k}^2 \, {\mathrm{RMS}_{PSF}}^2$$

Taking the square root we obtain an image RMS of

$$\mathrm{RMS} = \sqrt{\sum_{k=1}^{k} {I_k}^2 \, {\mathrm{RMS}_{PSF}}^2}$$

Because RMS_{PSF} is just a number that is only dependent on the PSF, and not on the source, we can take it outside the sum

$$\mathrm{RMS} = \sqrt{\mathrm{RMS}_{PSF}{}^2 \sum_{k=1}^{k} I_k{}^2}$$

And simplify to

$$\mathrm{RMS} = \mathrm{RMS}_{PSF} \sqrt{\sum_{k=1}^{k} I_k{}^2}$$

This equation is valid for isotropic, omnidirectional antennas. Of course, in reality, antennas are not positioned in free space and therefore have a position-dependent gain, so the actual result is:

$$\mathrm{RMS} = \mathrm{RMS}_{PSF} \sqrt{\sum_{k=1}^{k} G_k I_k{}^2}$$

where G_k is the antenna's gain towards source k. The above equation shows us three ways to reduce this contribution:

- Subtract more sources, so fewer contribute to the side lobe noise
- Reduce the PSF's RMS by creating a better filled synthesized telescope (uv-plane)
- Reduce the antenna's gain towards the interfering sources

What counts here in particular is the relative directivity, defined as the gain towards the wind turbine, divided by the mean gain across the rest of the hemisphere. Almost any antenna specifically selected for the task of measuring something at the horizon will have more gain towards the horizon than towards the sky, so for the example configurations we assume that the relative directivity of the antennas comprising the array is better than 0 dB. At 30 MHz, LOFAR's relative directivity for observing something at 6 degrees elevation is about -16 dB; excellent for observing the sky, but dreadful for determining the precise value of wind turbine emission at low elevations. We have to understand that there is a major difference between being hampered by faint signals entering one's instrument, and accurately measuring the powers of those faint signals.

For a sparse antenna array, the RMS and mean of the distant side lobe level are approximately 1/*N*, where *N* is the number of antennas in the array. The details, however, depend on the precise configuration. Having selected an antenna design, one therefore needs to add antennas to the configuration until the PSF RMS drops to an acceptable level. What is acceptable depends on how many sources can be subtracted well or at all.

Although simply subtracting all sources may sound appealing, there are limits to how well this can be done. The diffuse emission from the milky way is best removed by excluding all baselines shorter than 4 wavelengths from the imaging process, effectively spatially high-pass filtering the image. What remains are all the compact sources.

To distinguish these sources, there must be at least as many independent resolution elements on the sky as there are sources to subtract. Qualitatively, a resolution element corresponds to the main peak of the PSF. In practice, however, one needs

many more resolution elements on the sky than sources to subtract: In between the sources, there needs to be "empty" sky to prevent a noise floor due to all the unseen fainter sources (classical source confusion). The usual recommendation is to have at least 20 times more resolution elements (independent "pixels") than sources to subtract.

Every source that one solves for and subtracts, removes a degree of freedom from the imaging problem. The amount of available equations is equal to the total number of baselines, minus the baselines shorter than 4 wavelengths. Necessarily, the total number of sources to subtract must be (much) smaller than the number of useful baselines. Before source subtraction, however, we lose degrees of freedom by calibrating the array: 1 degree of freedom per antenna per direction for which we require a solution. We recommend to only calibrate for an overall gain/phase per antenna/receiver combination. In addition to that, we need to image the wind turbine. Because the required arrays are fairly large to deal with interference patterns from the wind turbine EMI onto the ground, the proposed array must have good spatial resolution, and requires several volume elements ("voxels") to image the wind turbine. This also costs as many degrees of freedom as there are voxels required. To err on the side of safety, we recommend to solve for and subtract at most a number of sources smaller than one third of the available degrees of freedom after removing the voxels covering the wind turbine, the calibration solutions per antenna, and all baselines shorter than 4 wavelengths.

The aim of the project effectively is to accurately measure the flux density of a source close to the horizon that is much fainter than the astronomical sources. The flux density measurement of the wind turbine is disturbed by the PSF side lobes of distant astronomical sources. The side lobes ending up on top of the turbine, that is. As is shown above, that noise term is linearly proportional to the RMS side lobe level of the PSF, where the PSF is the Fourier transform of the synthesized aperture (also called ‘uv’-plane) depicted in the top-right panel of the plots in Section 7.4. A fully filled aperture with uniform density makes the PSF equal to the Airy pattern (a J1 Bessel function) that is well known in optical imaging. A sufficiently uniformly filled aperture also allows tapering before imaging, reducing the far side lobes even further at the expense of slightly worse angular resolution.

The array shape that we propose is a Reuleaux triangle, which is the most asymmetric curve of constant diameter. It leads to an almost uniformly filled, circular synthesized aperture. The Reuleaux triangle has been used in several imaging-only radio interferometers before, such as the Sub Millimetre Array (SMA) on Mauna Kea, which uses several nested Reuleaux triangles. Different shapes such as circles, V-shapes and linear arrays were tested but produced a less uniform coverage, and therefore, more importantly, higher RMS side lobes and ultimately greater systematic errors. A Reuleaux triangle is easy to construct in a field using simple tools such as fixed-length ropes and wooden stakes.

Because this is a multi-dimensional problem with many possible solutions, we have run a large number of simulations, varying the antenna’s relative directivity, the number of antennas, and the array diameter. We then calculated the PSF RMS, and the number of sources to subtract to achieve the required noise level for a signal-to-noise of 10 for each emission level of the covenant, assuming a distance of 1000 m and a source height of 100 m.

To calculate the RMS due to not subtracted sources, we assumed a sky model consisting of the sources in the 3CR (Third Cambridge catalogue, Revised),

consisting of all compact radio sources brighter than approximately 10 Jy at 178 MHz. We assumed power-law radio spectra proportional to $\nu^{-0.7}$, [15] where ν is the observing frequency. Because half the sources are below the horizon at any time, we selected every other source, except for the brightest four, which we included in any case. We have subsequently selected configurations that had at least

- the number of antennas necessary to achieve the thermal noise;
- 20 times more pixels on the sky than sources to subtract;
- degrees of freedom remaining after calibration, wind turbine imaging, and source subtraction must be at least 2/3 of the useful visibilities after Fourier-filtering away the Milky Way;
- 3 times more degrees of freedom left after calibration than sources to subtract.

7.4 Practical lay-out

The antenna configuration mainly fulfils two different tasks: sufficient directivity in the direction of the interferer which is an object in the near field of the array at very low elevation angles and a sufficiently large footprint and number of independent baselines to provide data for the subtraction of celestial objects and interference which are in the far field at basically all elevation angles.
The distance of the array from the interferer is determined by the wavelength of the interference and the size of the interference "blobs" and the possibility to average them out over the size of the array. A distance of 1000m seems to be a realistic compromise with the sensitivity requirements and was used for the measurement campaign.

The ideal configuration for the first task seems to be a simple linear setup to achieve a good resolution in the direction of the wind turbine. When the antennas are 4λ spaced, in order to reduce galactic interference, for 30 MHz we need n-1 times 40 m for n antennas. This is 740 m for 20 antennas and leads to an unpractical configuration. However even with this configuration coverage of the galaxy is likely to be insufficient.

Based on the Reuleaux triangle extensive tables were produced for different frequency ranges, these are available but not included in this report. Compressed results for 30MHz are given in the tables 7.3 to 7.6 together with example configurations in Figures 7.5 to 7.8. It needs to be noted that the lowest frequency of 30 MHz basically defines the size and number of elements in the antenna array.

The top-left panel is the position of the antennas, in each case on the edges of Reuleaux triangles to yield an optimal filling of the synthesized imaging array (top right). Every point in the top right panels represents the position difference between a pair of antennas. The better filled this figure is, the better the final image quality will be. The red points in the top-right panels correspond to antenna pairs that are less than 4 wavelengths apart, and are not usable due to severe contamination by diffuse Galactic emission.

The middle right panels shows the point spread function (PSF), evaluated over twice the full sky to be able to calculate contamination from sources all the way at the opposite horizon. A lower side lobe level here implies better image reconstruction and less contamination from other sources of EMI (including cosmic sources).

The middle left panels show a histogram counting what fraction of the PSF has a lower level than "x" dB below the peak. It also shows the root-mean-square (RMS)

PSF levels, which can be used to calculate the image noise floor due to interfering cosmic sources that are not explicitly removed during the imaging and sky subtraction processing steps. The final contamination of the measurement of the wind turbine emission is linearly proportional to the RMS PSF level.

The bottom panel gives an impression what the configuration looks like from the direction of the wind turbine.

Number of antennas	array diameter (m)	directionality (dB w.r.t zenith)	sources to subtract -35	sources to subtract -40	sources to subtract -45	sources to subtract -50	pixels on sky	useful vis	degrees of freedom before source subtraction	voxels across turbine
12	200.0	0.0	3	6	37	137	1258	66	48	6
15	200.0	-8.0	10	89	155	165	1258	105	84	6
15	100.0	-4.0	5	19	118	161	314	87	69	3
15	150.0	-4.0	5	19	118	161	707	90	70	5
15	200.0	-4.0	5	15	110	159	1258	105	84	6
15	75.0	0.0	3	6	43	140	176	69	51	3
15	100.0	0.0	3	6	31	134	314	87	69	3
15	150.0	0.0	3	6	30	133	707	90	70	5
15	200.0	0.0	3	6	25	128	1258	105	84	6
18	100.0	-8.0	8	76	153	165	314	117	96	3
18	150.0	-8.0	8	70	151	165	707	135	112	5
18	200.0	-8.0	8	67	150	165	1258	135	111	6
18	75.0	-4.0	5	14	108	159	176	96	75	3
18	100.0	-4.0	4	11	99	157	314	117	96	3
18	150.0	-4.0	4	10	94	156	707	135	112	5
18	200.0	-4.0	4	10	91	156	1258	135	111	6
18	75.0	0.0	2	5	23	126	176	96	75	3
18	100.0	0.0	2	5	19	119	314	117	96	3
18	150.0	0.0	2	5	17	114	707	135	112	5
18	200.0	0.0	2	5	16	112	1258	135	111	6

Table 7.3: Possible configurations for a -35dB measurement

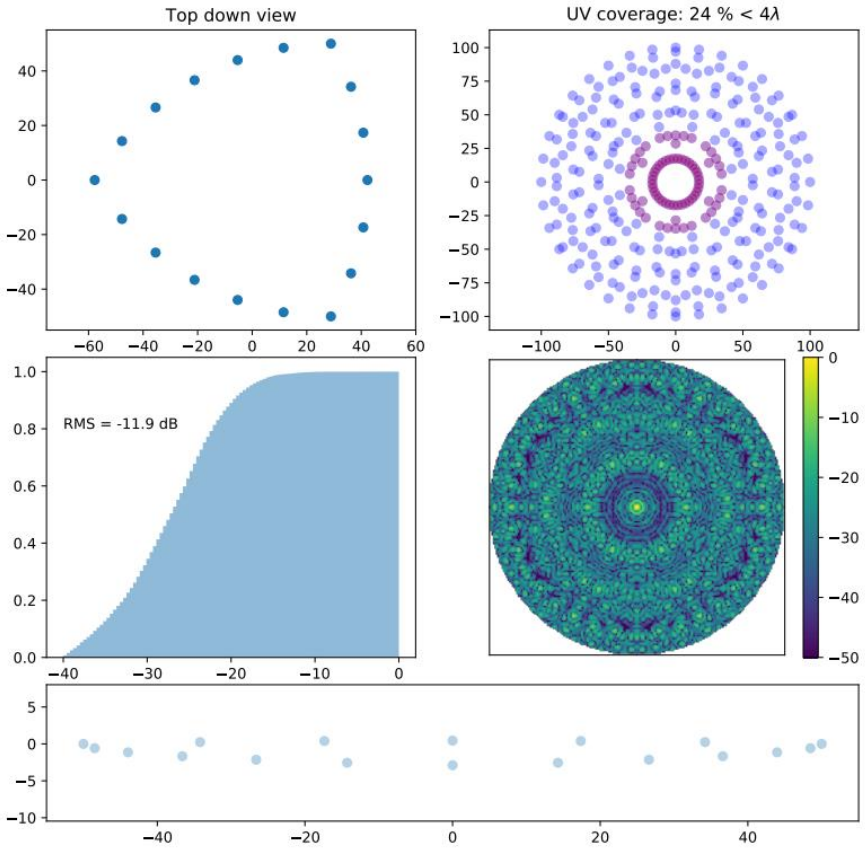

Figure 7.5: Array for -35dB measurements

Number of antennas	array diameter (m)	directionality (dB w.r.t zenith)	sources to subtract -35	sources to subtract -40	sources to subtract -45	sources to subtract -50	pixels on sky	useful vis	degrees of freedom before source subtraction	voxels across turbine
24	200.0	-8.0	6	41	139	164	1258	252	222	6
24	75.0	-4.0	4	8	75	152	176	174	147	3
24	100.0	-4.0	4	8	72	152	314	204	177	3
24	150.0	-4.0	4	8	60	148	707	228	199	5
24	200.0	-4.0	4	8	63	149	1258	252	222	6
24	75.0	0.0	2	4	11	99	176	174	147	3
24	100.0	0.0	2	4	11	96	314	204	177	3
24	150.0	0.0	2	4	9	84	707	228	199	5
24	200.0	0.0	2	4	9	87	1258	252	222	6
24	75.0	4.0	2	2	5	19	176	174	147	3
24	100.0	4.0	2	2	5	18	314	204	177	3
24	150.0	4.0	2	2	5	14	707	228	199	5
24	200.0	4.0	2	2	5	15	1258	252	222	6
24	75.0	8.0	0	2	3	6	176	174	147	3
24	100.0	8.0	0	2	3	6	314	204	177	3
24	150.0	8.0	0	2	2	5	707	228	199	5
24	200.0	8.0	0	2	2	5	1258	252	222	6
24	75.0	12.0	0	1	2	3	176	174	147	3
24	100.0	12.0	0	0	2	3	314	204	177	3
24	150.0	12.0	0	0	2	3	707	228	199	5

Table 7.4: Possible configurations for a -40dB measurement

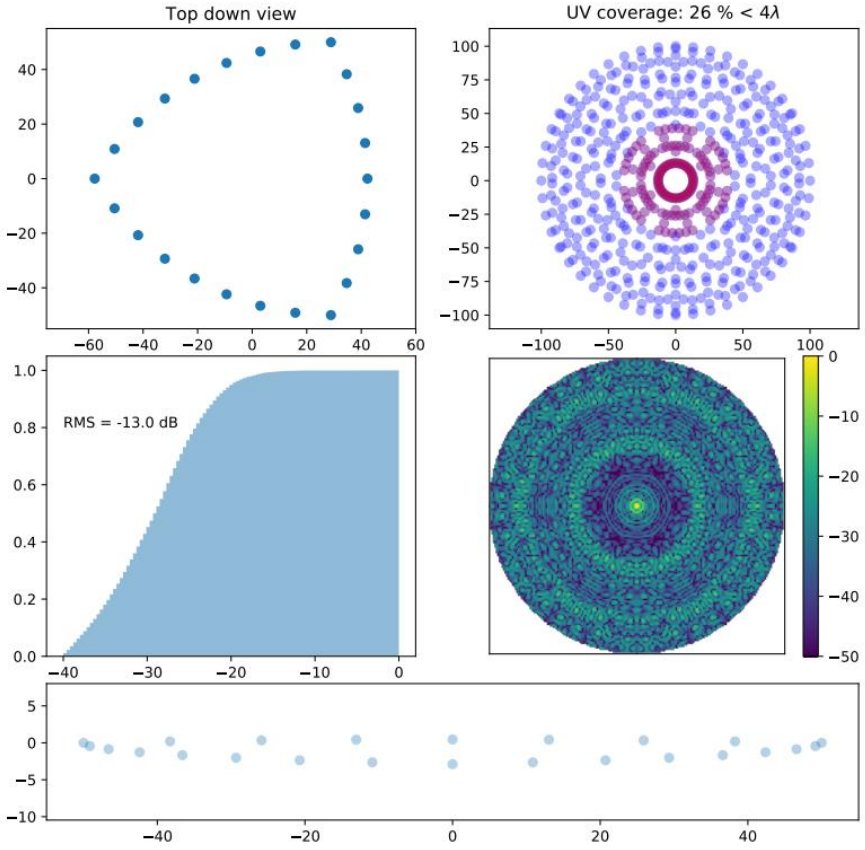

Figure 7.6: Array for -40dB measurements

Number of antennas	array diameter (m)	directionality (dB w.r.t zenith)	sources to subtract -35	sources to subtract -40	sources to subtract -45	sources to subtract -50	pixels on sky	useful vis	degrees of freedom before source subtraction	voxels across turbine
60	100.0	-4.0	2	4	13	104	314	1317	1254	3
60	150.0	-4.0	2	4	11	98	707	1461	1396	5
60	200.0	-4.0	2	4	10	92	1258	1581	1515	6
60	75.0	0.0	2	3	6	30	176	1107	1044	3
60	100.0	0.0	2	2	5	21	314	1317	1254	3
60	150.0	0.0	2	2	5	19	707	1461	1396	5
60	200.0	0.0	2	2	5	16	1258	1581	1515	6
60	75.0	4.0	0	2	3	7	176	1107	1044	3
60	100.0	4.0	0	2	3	6	314	1317	1254	3
60	150.0	4.0	0	2	3	6	707	1461	1396	5
60	200.0	4.0	0	2	3	6	1258	1581	1515	6
60	75.0	8.0	0	1	2	4	176	1107	1044	3
60	100.0	8.0	0	1	2	3	314	1317	1254	3
60	150.0	8.0	0	1	2	3	707	1461	1396	5
60	200.0	8.0	0	0	2	3	1258	1581	1515	6
60	75.0	12.0	0	0	1	2	176	1107	1044	3
60	100.0	12.0	0	0	1	2	314	1317	1254	3
60	150.0	12.0	0	0	1	2	707	1461	1396	5
60	200.0	12.0	0	0	1	2	1258	1581	1515	6
96	150.0	-8.0	3	6	25	128	707	3774	3673	5

Table 7.5: Possible configurations for a -45dB measurement

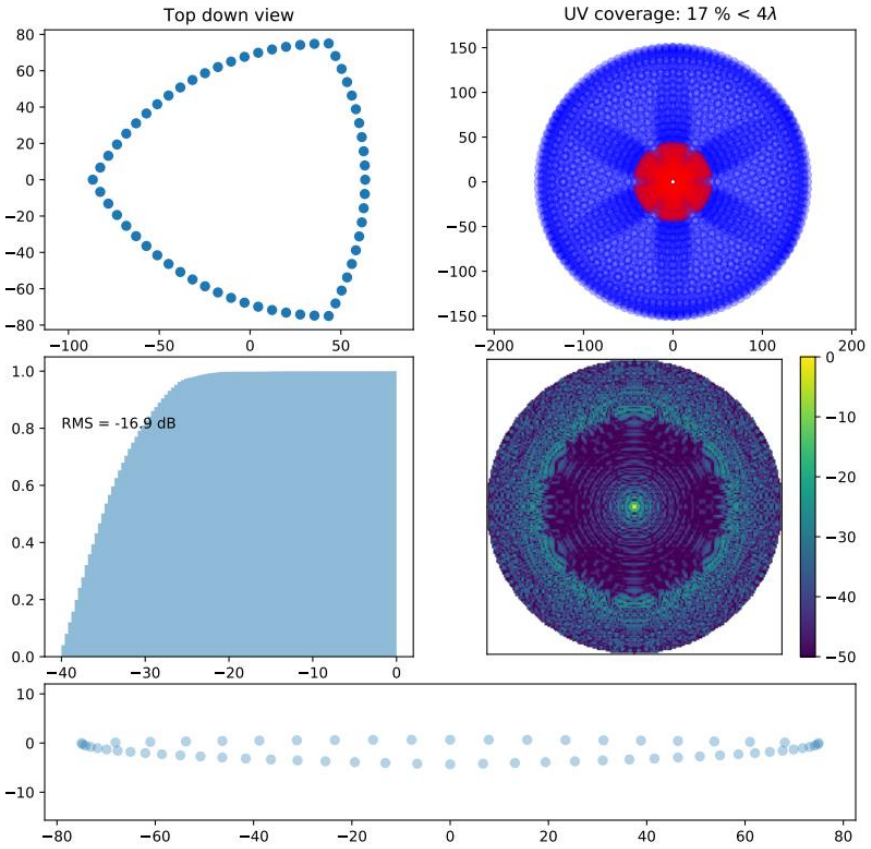

Figure 7.7: Array for -45dB measurements

Number of antennas	array diameter (m)	directionality (dB w.r.t zenith)	sources to subtract -35	sources to subtract -40	sources to subtract -45	sources to subtract -50	pixels on sky	useful vis	degrees of freedom before source subtraction	voxels across turbine
96	200.0	-4.0	2	3	7	59	1258	3972	3870	6
96	100.0	0.0	2	2	5	14	314	3339	3240	3
96	150.0	0.0	1	2	4	8	707	3774	3673	5
96	200.0	0.0	1	2	4	9	1258	3972	3870	6
96	75.0	4.0	0	2	3	7	176	2862	2763	3
96	100.0	4.0	0	2	2	5	314	3339	3240	3
96	150.0	4.0	0	1	2	4	707	3774	3673	5
96	200.0	4.0	0	2	2	5	1258	3972	3870	6
96	75.0	8.0	0	1	2	4	176	2862	2763	3
96	100.0	8.0	0	0	2	3	314	3339	3240	3
96	150.0	8.0	0	0	2	2	707	3774	3673	5
96	200.0	8.0	0	0	2	2	1258	3972	3870	6
96	75.0	12.0	0	0	1	2	176	2862	2763	3
96	100.0	12.0	0	0	1	2	314	3339	3240	3
96	150.0	12.0	0	0	0	2	707	3774	3673	5
96	200.0	12.0	0	0	0	2	1258	3972	3870	6

Table 7.6: Possible configurations for a -50dB measurement

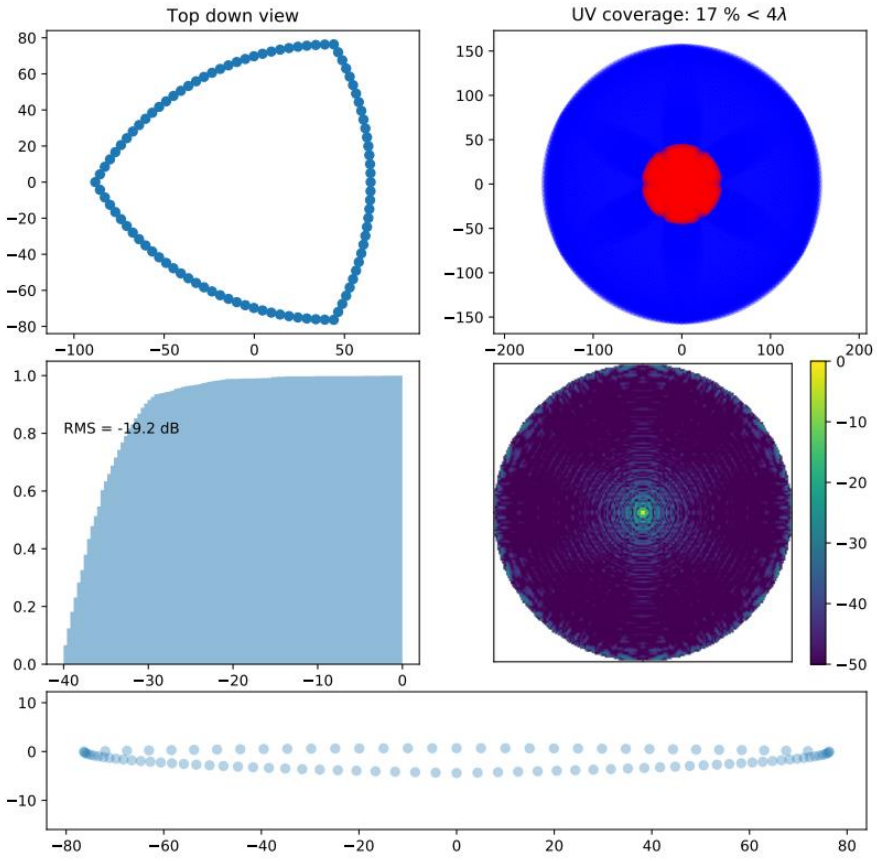

Figure 7.8: Array for -50dB measurements

The configuration with 96 antennas to measure the -50dB level seems large but we have to recognise the original LOFAR antenna consists of 48 double elements.

7.5 Suitability of the LOFAR stations and core stations for measurements

As stated earlier, there is a large difference between suffering an increase in systematic noise due to a source of interference, and measuring its flux density accurately at a signal to noise ratio of, for example, more than 10. Performing the same analysis on a LOFAR station using its 48 outermost low band antennas at 30 MHz, with a wind turbine at 1000 m distance and 100 m altitude, leads to the conclusion that one needs to subtract at least 60 sources to reach the -35 dB level. This is more than the 56 allowed before source confusion becomes important. The reason is that the LOFAR antennas have a relative directivity towards the wind turbine of approximately -15 dB: they are designed to observe the sky, not the horizon.

Using the core and a wind turbine at 5 km does in principle not improve this at first glance: the increase in sensitivity by having 24 stations is offset by the increase in distance by a factor 5.

Although the relative directivity is about 15 dB better per antenna station due to digital beam forming of all dipoles within a station (see the PSF / beam of an individual station), the RMS of the point spread function is worse because there are only 24 stations in a rather scattered configuration. These facts combined lead to the apparent need to subtract at least 55 sources to reach the -35 dB level. This is quite a lot, but not impossible. There is unfortunately a complication that does not exist in a station by itself: although all dual-dipole beams are fairly similar, the station’s digital beams can be rather different in the far side lobes through which the interfering cosmic sources shine. This means we need to estimate the beam gains in those directions as well, at least for the brightest few. This requires 24 parameters for each source to subtract: many more than the 276 useful cross correlations between stations, ruling out the core at first glance.

There is nevertheless an effect that we have not included in this analysis, which is the fact that for the core, the side lobes of the astronomical sources are much smaller spatially, and will move quickly across the wind turbine during the observation, decorrelating over time. This effect can become quite significant for the longer baselines, perhaps averaging out the effect of distant sources over the 1000 to 7200 seconds that an observation will have to take. This potentially requires one to subtract a much smaller number of sources. However, we have not yet performed that analysis quantitatively, so we can at this point neither confirm, nor rule out that the performance of the LOFAR core at 30 MHz is good enough to do the quantitative measurements required by the covenant.

The figures 7.9 and 7.10 for 24 LOFAR core stations and a LOFAR LBA outer station are included as illustration.

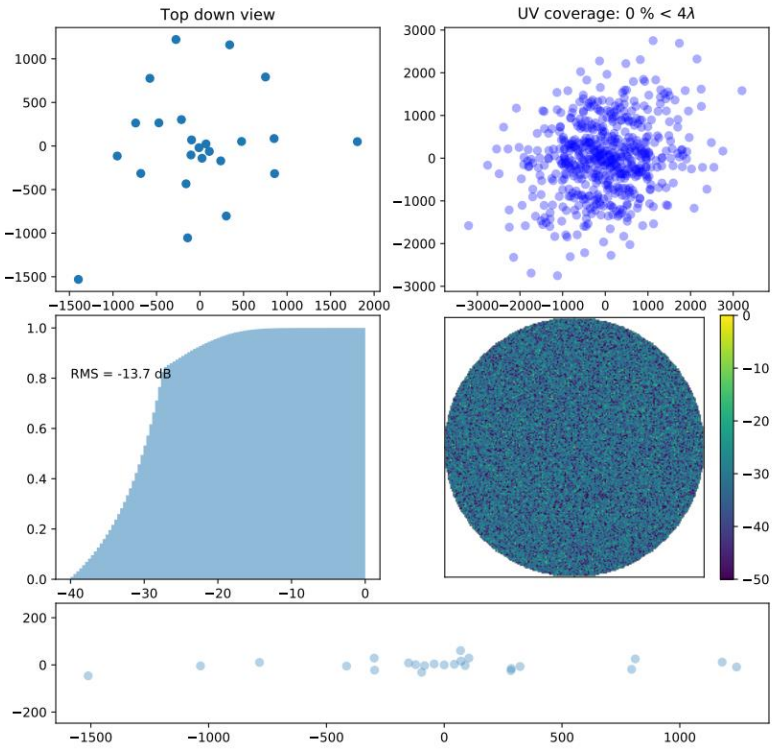

Figure 7.9: 24 LOFAR core stations

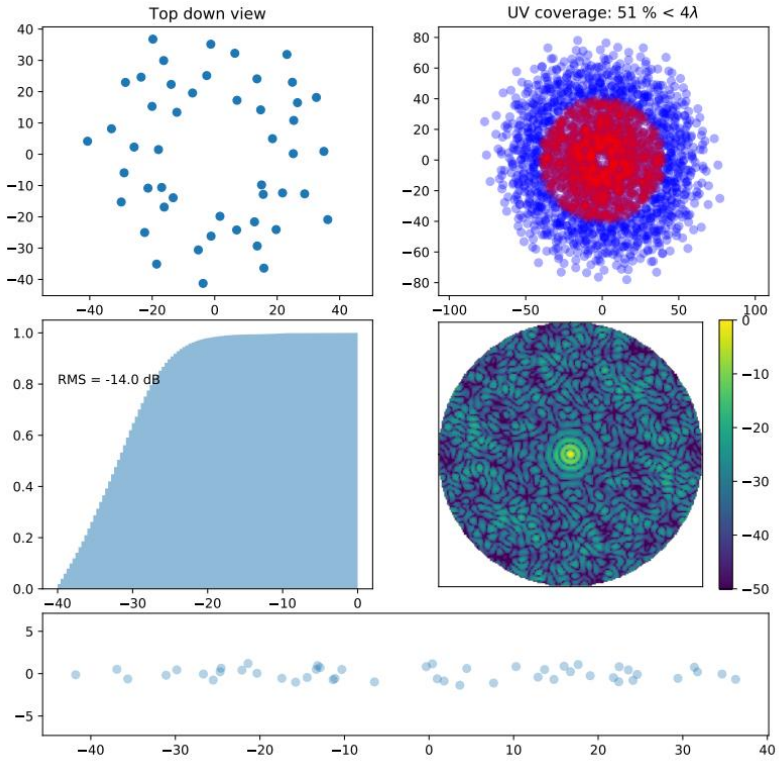

Figure 7.10: LOFAR LBA outer station

8 Conclusions and recommendations

This report describes a measurement method for measuring the extremely low levels of radiation that are required for wind turbines if they are installed in a distance of a few kilometers to the LOFAR core. These levels have to be extremely low because of the extremely high sensitivity of LOFAR. Nonetheless its high directivity towards space the high frequency radiation of wind turbines would interfere due to the side lobes of the antenna pattern. It has been pointed out in a previous report that the limits of the high frequency radiation of the wind turbines have to be 35 dB to 50 dB under the reference level based on CISPR11. Therefore they cannot be measured with usual measurement equipment and procedures. Standard equipment is much too insensitive and the measurement procedure is not exact enough.

The report proposes a different approach involving measurements with a an extended antenna array with a multichannel receiving system in about 1000 m distance and long integration times up to 2 h. The number of antennas and associated receivers, the dimensions of the array, and the integration time must ensure the required sensitivity and the need to subtract other interferers.
The other interferers are the "normal" EMI sources, but also the normal radio astronomical sky objects. Therefore both resolution in the direction of the wind turbine under test and the ability to remove unrelated interferers is required.

Due to the unknown path loss, for calibration purposes a calibrated source has to be mounted at a relevant position close to the wind turbine radiation sources. The measurement distance of 1000 m is a compromise between sensitivity and far field conditions.

A huge amount of data has to be digitized and stored of the received signals. Exact synchronization has to be assured. Only then the digital signal processing is possible.

This report describes the background, principles and validation of the recommended measurement method as required by the covenant. The implementation will require a separate engineering project with challenging choices, especially for the low frequencies.

8.1 Conclusions

Measuring the low EMI radiation from wind turbines in relation to the LOFAR radio telescope demands an array of multiple receivers and antennas and a software processing solution combined with a victim oriented approach. An array in the shape of a Reuleaux triangle has proven to be the most efficient configuration.

It turns out that the biggest technical challenge lies in measuring the lower frequencies (30-60 MHz) as can be seen in the table below.

Required level below norm value	Required # of antennas at **30 MHz** with array size D	Required # of antennas at **60 MHz** with array size D	Required # of antennas at **120 MHz** with array size D	Required observation time (s)
-35	18 (D=100 m)	18 (D=75 m)	18 (D= 75 m)	1000
-40	24 (D=100 m)	24 (D=75 m)	18 (D=100 m)	1000
-45	60 (D=150 m)	36 (D=75 m)	24 (D= 75 m)	1800
-50	96 (D=150 m)	60 (D=75 m)	36 (D= 75 m)	7200

Copy Table 1.1 number of antennas versus measurement level at 30, 60 and 120 MHz

Number of antennas
The number of antennas needed depends on the frequency that is being measured. For measuring the -35 dB level for the whole practical frequency band of LOFAR (30-240 MHz), a minimum number of 18 antenna elements with an array size of 100 m is required to obtain sufficient receiving sensitivity and the ability to filter out unwanted signals. The distance of the array from the wind turbine under test needs to be roughly 1000 m. The minimum observation time is 1000 seconds, provided appropriate antennas are used.

Measuring the -50 dB level down to 30 MHz involves about 96 antennas and 7200 s integration time with an array diameter of 150 m at 1 km distance, when we assume a directionality better than 0 dB and a gain towards the turbine better than -8 dBi for the antenna elements.

Type of antennas
The type of antenna has a strong influence on the number of antennas needed. This is shown in the table below for the aspect of antenna gain. All other things being equal, when the gain toward the wind turbine can be improved from the assumed -8 dBi to, for example -4 dBi the number of required antennas can be more than halved. The problem is that this improvement is not simple at 30 MHz.

Antenna dBi towards target	number of antennas -35 dB (1000 s)	number of antennas -40 dB (1000 s)	number of antennas -45 dB (1800 s)	number of antennas -45 dB (7200 s)	number of antennas -50 dB (1000 s)	number of antennas -50 dB (7200 s)
-12	20	63	148	74	626	234
-10	13	40	94	47	395	148
-8	8	25	59	30	250	93
-6	5	16	38	19	158	59
-4	4	10	24	12	100	37
-2	2	7	15	8	63	24
0	2	4	10	5	40	15
2	1	3	6	3	25	10

Copy Table 7.1 Required # of antennas as function of absolute gain in dBi

Use of LOFAR itself
It turns out that a LOFAR station by itself is not able to do certification observations all the way down to 30 MHz. The full LOFAR core may be able to do this, but to establish definitively whether this is possible requires more detailed simulation work.

Calibrated radio beacon
The method requires a calibrated radio beacon to ensure that any scalings of the absolute results due to local radio propagation peculiarities, antenna/receiver properties, and the data reduction method are measured and compensated for.

8.2 Recommendations for implementation

For a definite answer on the question whether or not the LOFAR core is suitable as a reliable instrument for measuring the EMI radiation of a wind turbine the authors recommend further research and detailed simulations.

Because LOFAR is built to observe the sky and its antennas are not optimized for measuring horizontally we recommend a semi-mobile solution with a dedicated antenna array for measuring wind turbines at the horizon.

A vertically polarised log-periodic antenna or other antenna with suppression in the direction of the zenith and high elevation angles, such as a (combination of) vertical monopole(s), is a suitable antenna element for a practical implementation. Using such an antenna element will aid in decreasing the number of antenna elements. It is up to a system designer to make a final choice when implementing the method, because bandwidth and observation time depends on the choice.

Because of the enormous relative frequency range, it may be economically attractive to work with more than one array, for example one from 30-80 MHz, and another one from 100-240 MHz.

References

1 “K-FACTOR calculations”, Ben Witvliet, Erik van Maanen, (26-09-2000, English version 17-10-2004)

2 Recommendation ITU-R SM.1753 Methods for measurements of radio noise

3 Report ITU-R SM.2055 Radio noise measurements

4 Practical Radio Noise Measurements; E. van Maanen; Radiocommunications Agency Netherlands; International Symposium on Electromagnetic Compatibility, Wroclaw, 2006.

5 Log periodic antenna design handbook; Carl E Smith; Smith Electronics; Cleveland Ohio 1966

6 Antennas, John D Kraus; McGraw-Hill 1988

7 Interferometry and Synthesis in radio astronomy, A Richard Thomson, James M Moran and George W Swenson; Krieger publishing company Malabar Florida 1988

8 Offringa, A. R. (2012). Algorithms for radio interference detection and removal Groningen: s.n.

9 Virone G., et al., “Antenna pattern measurement with UAVs: Modeling of the test source”, Antennas and Propagation (EuCAP), 2016 10th European Conference on, DOI: 10.1109/EuCAP.2016.7481744

10 Agentschap Telecom, ” Verstoring van het elektromagnetische milieu ter plaatse van de LOFAR kern door het wind turbinepark Drentse Monden en Oostermoer, Effecten op het Astronomie ontvangsysteem LOFAR”, 2016

11 Cornwell & Wilkinson (1981) "A new method for making maps with unstable radio interferometers" Monthly Notices of the Royal Astronomical Society, vol. 196, Sept. 1981, p. 1067-1086.

12 Bhatnagar (2013), "StefCal vs. Classical antsol: A critique", Personal Memo, http://www.aoc.nrao.edu/~sbhatnag/misc/stefcal.pdf

13 Donoho & Tanner (2009) "Observed Universality of Phase Transitions in High-Dimensional Geometry, with Implications for Modern Data Analysis and Signal Processing" arXiv:0906.2530 [math.ST] (DOI:10.1098/rsta.2009.0152)

14 The Low Frequency Array active antenna system, Gie Han Tan and Christof Rohner;

15 Cohen et al. 2004, "A DEEP, HIGH-RESOLUTION SURVEY AT 74 MHz", The Astrophysical Journal Supplement Series 150:417-430

16 Taylor, Carilli & Perley (1999) “Synthesis imaging in radio astronomy II”, Astronomical Society of the Pacific Conference Series, Vol. 180.

Annex A: Thoughts on implementation

Several methods of implementing and using the measurement system are possible. Implementation was not part of the investigation, but for the sake of completeness the different ideas that were discussed are described here.

Site survey
Before using a system like in section 3.3.6, it is necessary to perform a pre-test on the wind turbine and a site survey. This pre-test is used to make the actual measurement more reliable and also to save time in identifying beforehand possible measurement disturbances. It is advised to record as much as possible and make pictures of both the measurement setup and the turbine(s) under test and the situation during the test. The following list contains items minimal required in a site survey:

- Interference is not equally spread over the frequency band 30-240 MHz but is dominant at certain spots in the spectrum.
A wind turbine also doesn't radiate equal in all directions. Finding the "hot spots" in the frequency band and radiation direction of the interferer gives the possibility to focus on them and save measurement time in case of a suspected non approval condition. For approval the whole 30-240Mhz range needs to be measured.
- The exact position of the wind turbine should be recorded to aid later calculations in relation to the measurement system of which the exact location and orientation of the antenna elements should also be known.
- The position of local interferers in the measurement/observation bandwidth should be assessed, in particular the interferers located "behind" the wind turbine(s). In practice it is not possible to perform simultaneous measurements in different directions around the wind turbine(s), powering off the wind turbine(s) during site survey may be necessary. If interferers behind a wind turbine are not identified they may lead to false disapproval.
- Strong signals outside the measurement/observation bandwidth may cause blocking and intermodulation effect; these should be noted before and, if propagation is changing, during the measurements.

Antenna configurations
The obvious way to perform the measurements is to position the antennas at a distance required to guarantee that the radiated emission can be recorded and extracted from the data, assuming a particular observation time. This could be for example at 1000 m distance of the interferer at a particular angle. Another method proposed during discussions is to place the antennas in a circle around the interferer. This allows to "see" the wind turbine from different angles at the same time but introduces a challenge for both calibration and data processing; we do not advise to do this.

A designer needs to think about the practical layout of the system. All receivers could be placed in a single cabinet or constructed as self-contained receiver antenna combinations. In the first situation, long antenna cables are needed; in the second case, the receivers need to be synchronised using a, possibly, more complicated clock distribution system.
Also the level of EMI generated by this measurement system or people should be low compared to the distance emission under consideration. A mobile shielded room with all equipment integrated should be considered.

Separation in different components and operation
The measurement system can be separated in 4 different components, the antennas, the receivers, the data storage and the data processing unit including the software. In addition there is the calibration source consisting of a generator and an antenna. In principle the whole system has to be seen as a single unit but the logistics around its use may be different.
Before explaining the different possibilities, we need to understand that a measurement system as described in this report is not a "button operated" system that can be operated by any operator. The site survey, calibration and data analysis are specialised tasks.

- The often discussed way of use is a complete transportable system including all components listed above operated by skilled operator both installing the equipment and performing the measurements.

- It is tempting to separate the analysis from the actual data collection, so data collection may take place by less skilled operators and the analysis by more skilled personnel. Experience has shown this is possible in the case of routine measurements, but for more sophisticated tests in unique environments this may lead to invalid results. A quick quality check of data is needed in the field so separation of data collection and analysis is practical but always needs to be performed by skilled personnel. If the processes themselves are separated, more time can be spent on a better analysis. So some data reduction on-site may be possible, but a full analysis can be made afterwards at a different location.

- Another possibility is to separate the antenna system from the receiver and data collection part. If a semi-permanent antenna setup is used, several manufacturers may install their own antenna system at their own site but keep the receivers, data-collection and data-analysis as a separate part to be used by several users. This highly improves the speed at which a measurement can be made. An advantage is that transport and erection of relatively large antennas are not a limiting factor for the equipment anymore. There is some, maybe unfeasible, planning needed because of reasons given in the site survey paragraph. Also, by using commercial of the shelf devices and external data processing the system can be operational very quickly.

Wind turbine aging and enforcement issues
A large installation containing electronic equipment is subject to aging and modification/upgrades. It is therefore necessary to have a possibility to do an "on-site" measurement after the wind turbine is put into service. For enforcement purposes by the Radiocommunications Agency some of the implementation issues such as the permanent installation of an antenna system near the wind turbine are not always possible. Alerts given by the radio telescope itself are triggers for an investigation. The reaction to such a trigger from an enforcement point of view needs to be discussed however this is not part of the technical discussion about the measurement method and the placement of wind turbines but is mentioned here for the sake of completeness and also has a relation to article 8 of the covenant.

Annex B: Description of the test source, the UAV and the calibration

The used UAV is a hexacopter with a small beacon installed below. The radio frequency chain consists of a RF synthesizer, attenuators of different levels, and a vertically aligned wire antenna of different lengths loaded with weights to avoid movements as much as possible. The level of attenuators depends on the power mode (high-power or low-power) and on the frequency of the antenna under test (LBA or HBA), while the antenna length (1 or 2 meter long) depends only on the frequency of the antenna under test.

Fig B1 UAV and low band vertical

The generator is a comb generator based on a 6.25MHz oscillator and a harmonic generator. A combination of two lengths of wire for the antenna in combination with a decreasing power level versus frequency keeps the e.i.r.p within a 10dB range over the whole frequency range of the test, see figure B2.

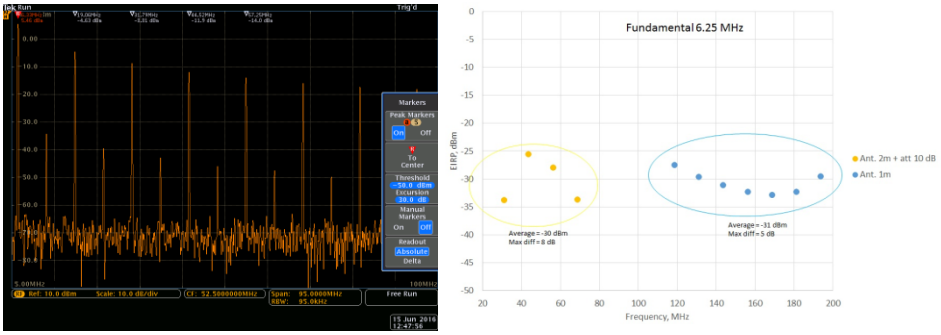

Fig B2 Spectrum and e.i.r.p. vs frequency

The estimation of the EIRP consists of both measured data, where possible, and simulated data. In particular, the simulations refer to the electromagnetic antenna characterization both in terms of mismatch loss and of pattern. This has been done by using FEKO EM simulation tool and implementing the wire antenna together with the UAV geometry (see Fig. B3); more info on this can be found in [8].

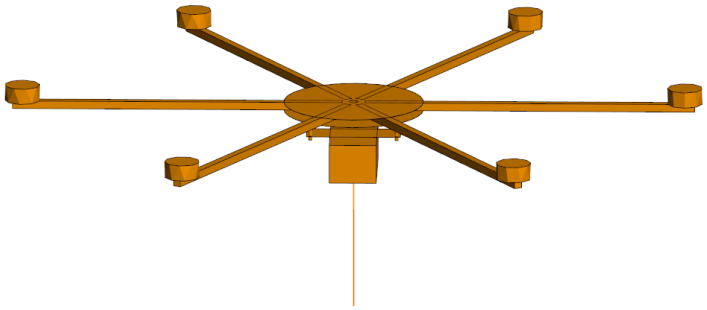

Fig B3 Geometry of the UAV plus antenna as implemented in FEKO

In addition, the most critical parameter, the antenna mismatch, has been also verified experimentally by using a reference antenna. The antenna matching is the most sensitive parameter being the antenna under test a monopole and therefore well matched only at the resonant frequency.

The e.i.r.p. is given for all the frequencies emitted by the UAV and at three different angles corresponding to the positions of the UAV with respect to the LOFAR station. However, it turns out that due to the large beam in the H-plane of the vertical monopole the e.i.r.p. values at different elevation angles are within 0.5dB (up to 1dB only at the higher frequency) and almost identical at different azimuth angles (not shown in the tables).

Four main contributions to the e.i.r.p. have been taken into account:

a. the power level at the output connector of the synthesizer → measured in the lab
b. the value of the attenuators introduced along the chain → measured in the lab
c. the mismatch of the antenna with respect to 50 ohm → simulated by FEKO and then verified on-the-field (see section on test procedure)
d. the antenna pattern along the desired directions → simulated by FEKO

Tables B1 and B2 summarize the e.i.r.p. computation for low-power and high-power mode respectively.

	Low power mode									
					Antenna pattern [dB] (simulated in FEKO)			EIRP [dBm]		
	Frequency [MHz]	Power from synthetizer [dBm] (measured)	Attenuation [dB]	Mismatch Loss [dB] (simulated in FEKO)	@ 93 deg (height 50 m, distance 1000 m)	@ 96 deg (height 100/50 m, distance 1000/500 m)	@ 101 deg (height 100 m, distance 500 m)	**@ 93 deg (height 50 m, distance 1000 m)**	**@ 96 deg (height 100/50 m, distance 1000/500 m)**	**@ 101 deg (height 100 m, distance 500 m)**
	31,25	-8,7	-46	-14,7	1,6	1,5	1,4	**-67,8**	**-67,9**	**-68,0**
	43,75	-11,7	-46	-0,1	1,9	1,9	1,8	**-55,9**	**-55,9**	**-56,1**
	56,25	-13,9	-46	-7,0	2,0	2,0	1,9	**-64,8**	**-64,9**	**-65,0**
LBA	68,75	-15,7	-46	-9,8	2,1	2,1	2,0	**-69,4**	**-69,4**	**-69,5**
	118,75	-20,41	-39	-8,4	2,0	2,0	1,9	**-65,8**	**-65,8**	**-65,9**
	131,25	-21,36	-39	-9,2	2,1	2,0	1,9	**-67,5**	**-67,6**	**-67,7**
	143,75	-22,3	-39	-9,6	2,1	2,1	2,0	**-68,8**	**-68,8**	**-68,9**
	156,25	-23,18	-39	-9,7	2,1	2,1	2,1	**-69,8**	**-69,8**	**-69,8**
	168,75	-23,97	-39	-9,3	1,9	2,0	2,1	**-70,4**	**-70,3**	**-70,2**
	181,25	-24,71	-39	-8,1	1,4	1,6	1,8	**-70,4**	**-70,2**	**-70,0**
HBA	193,75	-25,33	-39	-5,5	0,2	0,5	1,1	**-69,6**	**-69,3**	**-68,7**

Table B1 Computed e.i.r.p. low power mode

	High power mode									
					Antenna pattern [dB] (simulated in FEKO)			EIRP [dBm]		
	Frequency [MHz]	Power from synthetizer [dBm] (measured)	Attenuation [dB]	Mismatch Loss [dB] (simulated in FEKO)	@ 93 deg (height 50 m, distance 1000 m)	@ 96 deg (height 100/50 m, distance 1000/500 m)	@ 101 deg (height 100 m, distance 500 m)	**@ 93 deg (height 50 m, distance 1000 m)**	**@ 96 deg (height 100/50 m, distance 1000/500 m)**	**@ 101 deg (height 100 m, distance 500 m)**
	31,25	-8,7	-10	-14,7	1,6	1,5	1,4	**-31,8**	**-31,9**	**-32,0**
	43,75	-11,7	-10	-0,1	1,9	1,9	1,8	**-19,9**	**-19,9**	**-20,1**
	56,25	-13,9	-10	-7,0	2,0	2,0	1,9	**-28,8**	**-28,9**	**-29,0**
LBA	68,75	-15,7	-10	-9,8	2,1	2,1	2,0	**-33,4**	**-33,4**	**-33,5**
	118,75	-20,41	-3	-8,4	2,0	2,0	1,9	**-29,8**	**-29,8**	**-29,9**
	131,25	-21,36	-3	-9,2	2,1	2,0	1,9	**-31,5**	**-31,6**	**-31,7**
	143,75	-22,3	-3	-9,6	2,1	2,1	2,0	**-32,8**	**-32,8**	**-32,9**
	156,25	-23,18	-3	-9,7	2,1	2,1	2,1	**-33,8**	**-33,8**	**-33,8**
	168,75	-23,97	-3	-9,3	1,9	2,0	2,1	**-34,4**	**-34,3**	**-34,2**
	181,25	-24,71	-3	-8,1	1,4	1,6	1,8	**-34,4**	**-34,2**	**-34,0**
HBA	193,75	-25,33	-3	-5,5	0,2	0,5	1,1	**-33,6**	**-33,3**	**-32,7**

Table B2 Computed e.i.r.p. high power mode

Confidence of the e.i.r.p. values

An absolute measurement uncertainty analysis is not performed since most of the data in this section is obtained using EM simulation and no calibrated e.i.r.p. measurement is performed on all frequencies. However some cross checks have been performed on the data using the antenna patterns of the LOFAR LBA element. The cross checks found the e.i.r.p in agreement within 6dB of the simulated values. In our opinion this gives sufficient confidence the dataset is usable, but we have to keep this in mind for future development of the measurement system. In particular the calibration beacon needs, besides a simulation, a calibration on a suitable OATS (Open Area Test Site) to establish the uncertainty of its e.i.r.p and radiation pattern.

Annex C: Evaluation of a commercially available antenna

Evaluation of an alternative antenna element was not part of the investigation and a thorough test of such an alternative antenna has not been performed. However some test were performed during the measurement campaign and also some discussions took place. This antenna is therefore not specifically recommended but this section contains information that can be of use for someone developing a measurement system based on this report.

The LOFAR antenna elements are not the most suitable antennas for the final measurement system for several reasons. First they are split in a low band antenna and a high band antenna, making rapid mobile deployment impractical. Also the gain of the antenna under low elevation angles is very low. At 5° elevation the relative gain with respect to the gain in zenith direction is -20dB which means that strong noise from galactic objects is dominant in the registrations. A log periodic antenna overcomes such limitations if chosen carefully and may be used to improve the sensitivity of the system. The antenna in figure C1 shows such an antenna that was purchased to perform preliminary tests and pre-tests on installed wind turbines.

The antenna is manufactured by Alaris antennas http://www.alarisantennas.com/ , the type is LPDA-A0097. Specifications can be found here http://www.alarisantennas.com/products/wideband-wire-lpda-antenna/

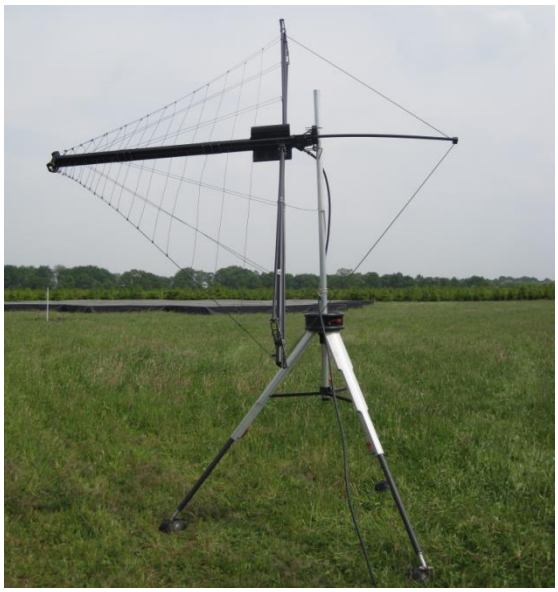

Fig C1 log periodic antenna LPDA-A0097

During the measurement campaign the antenna was erected at the same location as the LOFAR station used for the test. It was connected to a R&S FSMR spectrum analyser and a Mini Circuits ZX60-P103LN+ LNA with a gain of 25 dB and an OIP3 of 37 dBm at 50 MHz. To avoid interference during the tests, the equipment had to be switched off during the low power tests however the performance of such an antenna could be roughly estimated using the high power tests. Table C1 shows the

result of the high power test at 1000 m distance for both 50m and 100 m height. The SN ratio of the received power and the receiver noise floor in 100 Hz bandwidth is also given.

Distance=1000 m	Altitude 50 m		Altitude 100 m	
Frequency [MHz]	Level [dBm]	SN ratio [dB]	Level [dBm]	SN ratio [dB]
31.25	-103	38	-101	40
43.75	-93	47	-90	50
56.25	-101	40	-97	43
68.75	-105	35	-102	38
118.75	-120	23	-117	30
131.25	-115	27	-114	32
143.75	-117	25	-115	32
156.25	-120	21	-120	27
168.75	-117	25	-117	30
181.25	-111	30	-115	33
193.75	-110	31	-115	33

Table C1 Received signal levels and signal to noise ratios in a 100Hz bandwidth of the high power test at a distance of 1000m and heights of 50 and 100m

The antenna was positioned on a tripod and slanted for practical reasons. Since the generated signal was vertically polarised there is some additional insensitivity.

The test signal is clearly visible in all cases, for the low band on an average of 40dB and for the high band 30dB above the noise floor of the receiver. A signal with the -35dB relative level would be detectable for the low band with a single antenna but not for the high band provided that the signal is narrowband (<100 Hz). For real signals with a larger bandwidth than 100 Hz a single antenna element cannot be used as already explained in annex E.

As already mentioned one important factor to be taken into account is the directivity towards the zenith and the interferer. A large part of the processing method is based on the elimination by filtering of interferers which are present in the sky. An antenna system with a suppression towards the sky and some gain in the direction of the interferer is preferred over an antenna with a large overall omnidirectional gain. Figure C2 shows the radiation pattern of both the LOFAR LBA element and the LPDA-A0097 log periodic antenna at 1,5 m above ground at 50 MHz.

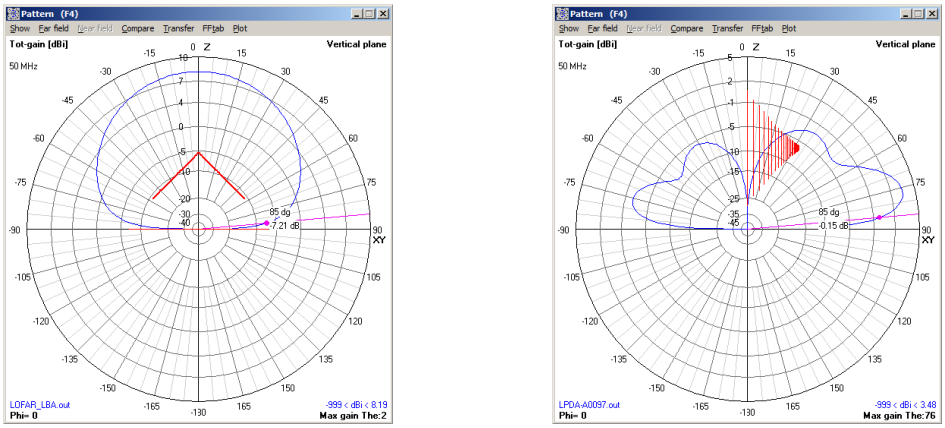

Fig C2 Vertical antenna patterns, total gain of LBA antenna and log periodic antenna LPDA-A0097 at 50 MHz

The patterns are plotted in the direction of the max vertical gain. Average ground was used for the ground model; a patch was used for the LBA groundplane.

NOTE: In previous simulations and calculations for the processing of data for this experiment simulations were performed in the direction of antenna as used during the experiment. This results in a slightly lower gain at low angles for the latter.

Considering the gain of the log-periodic antenna and its radiation pattern the antenna was found suitable for a future measurement system provided the antenna pattern is determined for the whole frequency range. This pattern is dependent on the height above ground vs the frequency so multiple measurement heights may be necessary.

As already said, this LPDA antenna is just an example of a commercially available antenna. Other antennas such as vertical monopoles might also be applicable. A similar analysis needs to be made for any other type of antenna to be used in the measurement system.

Annex D: Receivers

For the choice of the receiver the original LOFAR receiver can be used as a guideline. These receivers are not overdesigned and offer therefore a cost effective solution.

These employ 12 bit AD converters, representing a theoretical dynamic range of 72dB. The sensitivity of these AD converters is -139dBm/Hz.
Direct after the antenna element an amplifier (LNA) is placed. The antenna amplifier cable combination sensitivity is defined in terms of noise temperature in percentage skynoise. Table D1 indicates the current values for the Low and High band antenna.

	LBA (30-90 MHz)	HBA (110-170 MHz)	HBA (170-250 MHz)
Actual ADC dynamic range	60 dB	60 dB	60 dB
ADC noisefloor	-139 dBm/Hz	-141 dBm/Hz	-140 dBm/Hz
Preamplifier gain	25 dB	22 dB	27 dB
Noise density@ input receiver	-164 dBm/Hz	-169 dBm/Hz	-167 dBm/Hz
Noise figure	10 dB	11 dB	13 dB
OIP_2	>41 dBm	>51 dBm	>45 dBm
OPI_3	>26 dBm	>19 dBm	>16dBm
Noise temperature % skynoise	<20%	<=100%	<=100%
NOTE: No measurements are performed in the FM broadcasting band			

Table D1 Current realised LOFAR receiver specifications

If antennas with significantly more gain towards the wind turbine are used lower gain values for the preamplifier can be specified. More information on a predesign of this amplifier can be found in Tan and Rohner [14].

The following is meant to be a starting point for further research:

A possible receiver mentioned during the discussions is the USRP X310 van Ettus Research. https://www.ettus.com/product/details/X310-KIT Some of this equipment is also available from and supported by national instruments
This receiver needs one daughterboard for each receiving channel needed in order to operate from 1-250 MHz https://www.ettus.com/product/details/BasicRX
An external anti-aliasing filter and a preamp with sufficient gain and linearity also needs to be installed.
For clock distribution a standard solution for 8 outputs is also available.
https://www.ettus.com/product/details/OctoClock-G
This receiver may need modifications in order to make it applicable in a measurement system. Other receivers might be applicable as well.
Also here special care should be taken about dynamic range, sensitivity and stability.

Another possible receiver is the IZT R5000 from IZT https://www.izt-labs.de/en/products/category/receivers/product/izt-r5000-1/
This receiver is available as building block for system integrators

Cost effective solutions are the blade rf https://www.nuand.com/
or the spectrum analysers from signal hound https://signalhound.com/
and aaronia http://www.aaronia-shop.com/products/spectrum-analyzer/real-time/customizable-spectrum-analyzer

Possibility to synchronise multiple analysers and realtime bandwith need to be investigated. These devices may need a frequency converter to achieve the full frequency range.

Annex E: Rejected measurement methods

Using the data from the previous sections different scenarios for a possible measurement method are proposed. It was clear from the beginning that not all of these proposals are practical or achievable, but they are mentioned to have a complete overview of what was discussed in the project team.

Near field scan

A near field scan is a multipoint measurement of radiated power at a short distance from which the radiated power at a larger distance (in the far field) can be derived. This is a method often used for measurements on large antennas where for example the antenna diagram cannot be practically measured in the geometric far field. When employing such a scan it is required to know the phase and amplitude of the individually measured components.

When measuring the radiation from a wind turbine the phases of the individual components are not known and also not phase coherent. We also have to scan an estimated vertical plane of 100 m x 50 m at an operating wind turbine which implies serious safety considerations. The near field scan also needs to be performed in such a way that all points in this plane are measured in a time interval in which the radiation pattern doesn't change, (near real time). A near field scan is therefore not possible from a practical point of view.

Besides the fact that **a near field scan is not possible from a practical point of view** it is also not possible to measure amplitude and phase in real time.

Regular EMC approach

The regular EMC measurement is a near field measurement in a single point or using a, sometimes limited, height scan and has the same limitations as the near field scan due to the mechanical size of the radiator. In contrast to a near field scan or far field measurement an EMC measurement lacks the possibility to include, partly or in full, the dynamic effects of the rotating blades of the wind turbine. A single EMC measurement therefore does not give insight in the effect of the most important interference mechanism. A sequence of EMC measurements at different points, possibly at short distance, may give a better result about the dynamic behaviour but here we also have the limitations of the near field scan. An absolute field strength measurement is not possible since it is not possible to compensate for the field strength interference pattern as described in section 6.2.

It is possible to investigate the emissions from a wind turbine from a very short distance or inside the windturbine, even with portable equipment, to identify the main emission sources. Also the main interfered frequencies can be identified. This may be useful during a pre check but has ofcourse no relation with any e.i.r.p. value or value from the covenant.

The method **does not fulfil the requirements of an absolute field strength measurement** however the method can be used during a pre check to support corrective actions.

When we reduce the measurement distance we encounter similar issues as with the near field scan and the EMC method but in a less problematic form. No statement however can be made about the absolute field strength.
At short distances it is not possible to perform a meaningful field strength measurement as with the EMC method but at larger distances this is possible. It is therefore necessary to measure outside the first Fraunhofer region, but there is a frequency limitation of what can be measured and what not. See table 1 for some distances related to the frequency, at 75MHz the required distance is already too far to perform a field strength measurement with standard equipment.

The method **does not fulfil the requirements of an absolute field strength measurement** for the entire frequency range.

Standard measurement equipment and the application of decimation and processing

Decimation based on Cascaded Integrator Comb (CIC) filtering can increase the dynamic range with multiple bits resulting in about 30-40dB based on a decimation with a factor 100. It is therefore necessary to record the signal broadband in IQ format and to process it. There is a possibility to do this in "real time", but for cost reasons it is more attractive to store the data and perform the processing offline. An advantage is that we can use cost effective off the shelf equipment and the processing is also relatively cheap. There are two disadvantages. Decimation has a limited possibility to increase sensitivity so the measurement distance is still within the near field region. Because of the processing there is a chance that the dynamic nature of the interference is lost. In combination with a high gain Low Noise Amplifier (LNA) this option might be a possible solution for the sensitivity issue but not for the complications associated with a near field measurement. This means that this method cannot be performed with a single receiver and antenna setup.

Because of high cost and the very limited possibilities compared to the method in section 3.3.6, it was decided not to further develop this method.

Standard measurement equipment and cross correlation

This method needs two coherent receivers and two antennas; one antenna is pointed at the interference source and the other is pointed in a different direction, not too far off the direction of the interfering source.
Cross correlating the signals of both receivers lowers the noise floor about 10dB. An oscilloscope or computer may be used as indicator.
The method cannot be used as an absolute field strength measurement method since it is not possible to compensate for the field strength interference pattern as described in section 6.2.
The method is extremely frequency sensitive so only narrowband measurements are possible without recalibrating the setup. The directivity of the antennas and the actual presence of interferers has a large effect on the applicability of this method.

The method **does not fulfil the requirements of a calibrated field strength measurement**.

Annex F: Validation experiment

The first step to come to a practical solution after the analysing the design criteria is to generate a test signal to be received with all 48 antenna pairs in one of the LOFAR core stations. In order to test the necessary number of antennas and the development of the measurement and analysis algorithm a drone was used to simulate the -35dB reference level agreed in the covenant. With this level it is also possible to verify the theoretical calculated number of antennas required to obtain higher sensitivities such as -45 and -50 dB below the reference level. Two levels were generated, the 0dB level of the EMC standard EN55011-A1 and the actual covenant level which is 35dB below this level. The used frequencies were 31.25, 43.75, 56.25, 68.75, 131.25,156.25, 168.75 and 181.25 MHz. Each was observed in a 170 kHz subband. For this reason the power level generated was set to the values in table F1. An additional 3 frequencies were used in the high band to check the log periodic antenna.

	P e.i.r.p.	P e.i.r.p. (dBm)	Equivalent flux density @ 600m in 170 kHz	Equivalent flux density @1000m in 170 kHz
Ref level	0,47 µW	-33,2	61 MJy	22 MJy
-35dB level	0,15 nW	-68,2	19 kJy	7 kJy

Table F1 Power levels for the test

As can be seen in the table, the generated signal level is compensated for by the 170 kHz observation bandwidth. Since in principle all power may be spread over the whole 170 kHz bandwidth, this signal is significantly higher than the values in figures 6.3 and 6.4.

The LOFAR antenna field used in the test consists of crossed antenna elements providing two perpendicular polarisations to the azimuth. The field consists of a low and high band section, therefore the test was split in a separate 30-70 MHz and 70-200 MHz test. The low band section consists of inverted V's used as a single element and the high band section of elements combining 16 element bow tie antennas. In the 16 element bow tie section only one element was used to provide a better low angle sensitivity.

The drone was flown at 4 different positions: two different distances 1000 m and 500 m and two different heights 100 m and 50 m. The flights were split in a HBA and LBA part and performed on two different days, see table F2 for details.

Generator level relative to EMC reference level	1000 m Day-3	1000 m Day-2	500 m Day-2	500 m Day-3
0 dB	LBA	HBA	LBA	HBA
-35 dB	LBA	HBA	LBA	HBA
-∞ dB	LBA	HBA	LBA	HBA
0 dB	-	-	LBA	HBA

Table F2 Power levels for the test

The 0dB level is used for absolute level calibration. For the final measurement setup a similar calibration source with known e.i.r.p. in the direction of the measurement setup is needed. This source does not need to be drone deployed but can be placed for example on the nacelle or the tower of the wind turbine.

Besides the two signal levels a sanity check was performed using the drone with connected antenna, and installed beacon but without powering the beacon. This was for assessing the possible EMI radiation from the drone itself.

To achieve sufficient sensitivity to detect the agreed upon maximum emission levels from wind turbines at approximately one km away, one requires multiple antennas as described in section 6. Clock synchronisation and time distribution of ADC's is required and data needs to be time-tagged (in our case in UTC).

The primary data consists of complex voltage (I/Q) data from every single antenna. The bandwidth per data stream could be anything from 1 MHz to the full 220 MHz. In our case we used four, 170 kHz bands in the low frequency range and 4, 170kHz bands in the high frequency range (a total of 8 bands).

The measured data was processed offline and imaged to check the level and direction of the emission. The signal processing steps are described in detail in section 6.

This section will be completed in the future with more information from the measurement campaign.

Revision table

Version	Date	remarks
0.19	12-07-2017	First internal review
0.29	31-07-2017	Major restructuring, substantial additions, second internal review
0.90	08-08-2017	Final version for external review
0.91	23-08-2017	Modified based on external review
0.92	29-08-2017	Modified based on external and internal review for check
0.93	04-09-2017	Update with check reviewers
0.94	06-09-2017	Conclusions and recommendations added; typos.
0.95	07-09-2017	Added Reuleaux explanation, new Table 7.3; typos
0.96	08-09-2017	Extended Table 1.1, final edit Ch.8
1.00	08-09-2017	Final version for coordination committee